

Magmatic and tectonic continuous casting in the circum-Pacific region

Jon E. Spencer

Arizona Geological Survey, 416 W. Congress St., #100, Tucson, Arizona, 85701, USA

Yasuhiko Ohara

*Hydrographic and Oceanographic Department of Japan, Tokyo, 104-0045, Japan, and
Institute for Research on Earth Evolution, Japan Agency for Marine-Earth Science and Technology,
Kanagawa 237-0061, Japan*

ABSTRACT

Continuous casting is an industrial process for producing metal in continuous linear form. Cooling of the cast medium occurs across a slip surface in this process. The same process was active in geologic settings in which lava extrusion was accompanied by formation of striations on the surface of the extrusion. Such grooves resulted from irregularities on colder and harder rock that formed the confining orifice from which the grooved lava was extruded. In a variant of this process, lavas that emerged from beneath deep-sea lava-lake crusts were striated on their upper surfaces as they emerged. In the case of the grooved extrusion at Sacsayhuamán, Perú, lateral displacement of rock overlying a very shallow intrusion may have caused striations to form on the underlying intrusion as it was exhumed.

Deep-sea metamorphic core complexes are known primarily by their corrugated upper surfaces as identified with multibeam sonar. Recovered samples, including from drilling, typically include gabbro and basalt, indicating that magmatism was a major process in construction of the corrugated normal-fault footwall. The 125-km-long Godzilla Mullion in the Parece Vela Basin of the Philippine Sea, which is the largest known metamorphic core complex on Earth, includes a single antiformal groove 60 km long and 5 km wide. As with all deep-sea core complexes, grooves are parallel to nearby transform faults and to plate spreading direction. Tectonic continuous casting beneath a corrugated fault surface is the only known process that could produce such long grooves. Abrupt terminations and changes in groove form were likely due to incision and excision in which fault slivers were transferred from one side of the fault to the other, thereby changing the shape of the hanging-wall mold and cast footwall.

One of the major insights in identifying processes of continental lithospheric extension is that the deep crust, or “fluid crustal layer,” is sufficiently mobile because of quartz crystal plasticity that it gradually flows in response to lateral pressure gradients. Large-displacement normal faults known as detachment faults have uncovered this fluid crustal layer in the mylonitic footwalls of continental metamorphic core complexes. Some core complexes are grooved over tens of kilometers, with grooves parallel to extension direction. While these grooves were likely produced by tectonic continuous casting, it has not yet been demonstrated that molding actually occurred. Examples of corrugated normal faults, or of exceptionally long or well developed grooves that were plausibly produced by tectonic continuous casting beneath corrugated normal faults, include the Wasatch front in Utah, Rincon Mountains and Harcuvar-Buckskin Mountains in Arizona, Dayman dome in Papua New Guinea, and the Pompangeo Mountains of central Sulawesi in Indonesia. These five areas are described to illustrate the evolution from corrugated range-front normal fault to corrugated metamorphic core complex.

key words: *core complex, continuous casting, grooved lava, detachment fault, normal fault*

e-mail: Spencer: jon.spencer@azgs.az.gov; Ohara: yasuhiko.ohara@gmail.com (also at: ohara@jodc.go.jp)

Spencer, J.E., and Ohara, Yasuhiko, 2008, Magmatic and tectonic continuous casting in the circum-Pacific region, *in* Spencer, J.E., and Tittley, S.R., eds., Ores and orogenesis: Circum-Pacific tectonics, geologic evolution, and ore deposits: Arizona Geological Society Digest 22, p. 31-53.

INTRODUCTION

“If the casting is to have external ribs, the shaping wall of the mold must also be appropriately ribbed.” (Herrmann, 1980, Handbook of Continuous Casting, p. 115).

Continuous casting is a widely used industrial process for converting molten metal into continuous linear forms, typically with a square or rectangular cross section. Unlike conventional casting, the interface between mold and cast medium is a slip surface. The essential element in the process is cooling and solidification of the cast medium during extrusion from a mold. Continuous casting gained wide use in middle to late 20th century because it allowed much greater production rates than conventional incremental casting. The highest extrusion rates are obtained where the outer, solidified part of the extruded medium is just strong enough to contain a still-molten core without deforming (Figs. 1A, B; Herrmann, 1980; Tselikov, 1984).

The basic process of continuous casting was vaguely recognized more than a hundred years ago as applying to a striated lava extrusion, but was not given a specific name (Hovey, 1903). Since then it has been repeatedly recognized in diverse magmatic settings. Tectonic continuous casting has been proposed more recently for formation of corrugations on metamorphic core complexes where groove formation would have occurred over $\sim 10^5$ - 10^7 years (Spencer and Reynolds, 1991; Spencer, 1999). In industrial continuous casting and some magmatic continuous casting, the extruded medium is entirely surrounded by a slip surface, whereas in tectonic continuous casting only one side of the extruded medium is bounded by a slip surface while movement is accommodated elsewhere by divergence of crustal blocks or tectonic plates. Although much slower than magmatic continuous casting, the essential process of molding and shaping of a hot, plastic medium (the core complex) during extrusion from beneath a colder, stronger medium (the hanging-wall block of the normal fault bounding the core complex) appears to be the same. In both magmatic and tectonic continuous casting, the grooves reflect the form of the colder and harder molding rock. Controls on groove wavelength and amplitude remain poorly understood, but appear to represent the initial irregularities of a newly formed fracture or fault surface modified by smoothing due to transfer of magma or rock from one side of the slip surface to the other.

The circum-Pacific region contains many if not most of Earth's best examples of grooved lavas and corrugated core complexes. This paper reviews some of those features, presents color photographs of grooved lavas and color images derived from digital elevation models of grooved core complexes, and discusses issues surrounding groove genesis and evolution. Understanding of groove genesis in metamorphic core complexes is still tentative and remains a challenge to structural geologists.

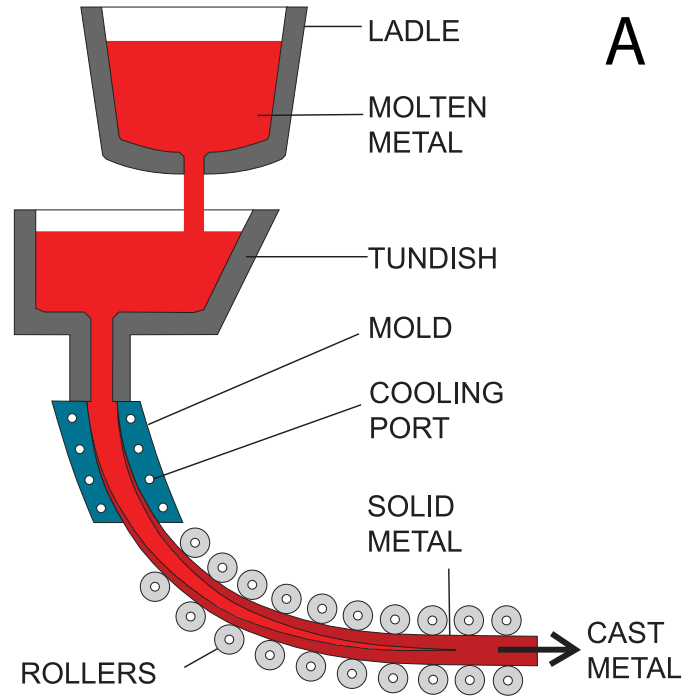


Figure 1. (A) Cross section of a continuous-casting machine for steel production (modified from Tselikov, 1984). (B) Photograph of continuously cast steel immediately following extrusion from the mold.

MAGMATIC CONTINUOUS CASTING

Continuous casting occurs naturally in magmatic settings where magma is shaped, cooled, and hardened during igneous extrusion. Grooves on extruded lava in a variety of geologic settings have been interpreted as products of abrasion during extrusion or during exhumation from a position beneath or adjacent to solid rock. The great length of some

grooves, with groove width a tiny fraction of groove length, requires a large strength contrast between the soft, grooved medium and the hard, abrading rock. The remarkable length of such grooves at Sacsayhuamán (Perú) was interpreted by Feininger (1980) to indicate that abrasion along a slip surface could not have produced the grooves because the abrading medium would be worn flat by the abrasion process and the grooves would fade along groove length. This view, however, fails to consider the enormous strength contrast that is possible where viscous magma is just cool enough to maintain the form of grooves produced by abrasion against colder and much stronger solid rock.

For example, the tops of some very young lava flows such as the Holocene Bonito Flow adjacent to Sunset Crater in northern Arizona (USA) are marked by fissures containing upward-pointing, wedge-shaped rock bodies with striated sides (Fig. 2A). Striations range from a few millimeters to less than a millimeter across, yet are continuous over lengths that are hundreds of times greater than groove width (Fig. 2B). These striated wedges have been interpreted as lava “squeeze-ups” in which lava was extruded from the flow interior as the flow-crust fissure widened. Striations on the sides of squeeze-ups are interpreted as reflecting the “plastic” or “stiff clay” like character of the lava as it was abraded by the adjacent hardened lava crust during extrusion (Colton and Park, 1930; Nichols, 1938). This interpretation is supported by images of striated surfaces broken into fragments that remain firmly attached to the solidified interior of the squeeze up, as if the exterior of the squeeze up had become sufficiently solidified to behave somewhat brittlely while the interior remained soft (Fig. 2C).

McCartys flow in the Zuni-Bandera Volcanic Field of western New Mexico (USA) is characterized over several percent of its surface by lava-crust fragments that “are turned up on end and capsized like cakes of ice in an ice jam” (Nichols, 1938, p. 601). Many fragments are vesicular on one side and grooved on the other, or are less vesicular on the grooved side. Nichols (1938) interpreted the grooves to have formed during lava-flow emplacement when the solid crust fragmented during lava flow and the fragments, with molten undersides, were scraped against each other, one overriding another. In this situation, lava is not extruded from a crack or orifice, analogous to industrial continuous casting, but rather is scraped and shaped on one side as the other side adheres to the solid lava fragment. However, the essential process of continuous casting, in which cooling, hardening, and shaping occur in the presence of a high thermal gradient across a slip surface, is the same.

Deep marine basalt eruption is characterized by somewhat different physical behavior than subaerial eruption because sea water is much more effective at quenching emerging lava and because great pressure prevents vesiculation. Photographs taken from deep-diving vehicles have revealed lineated basalt-flow tops, especially at the Young Sheet Flow on Juan de Fuca Ridge in the northeast Pacific where about 0.7 km² of sea floor are covered by remarkably lineated, recently

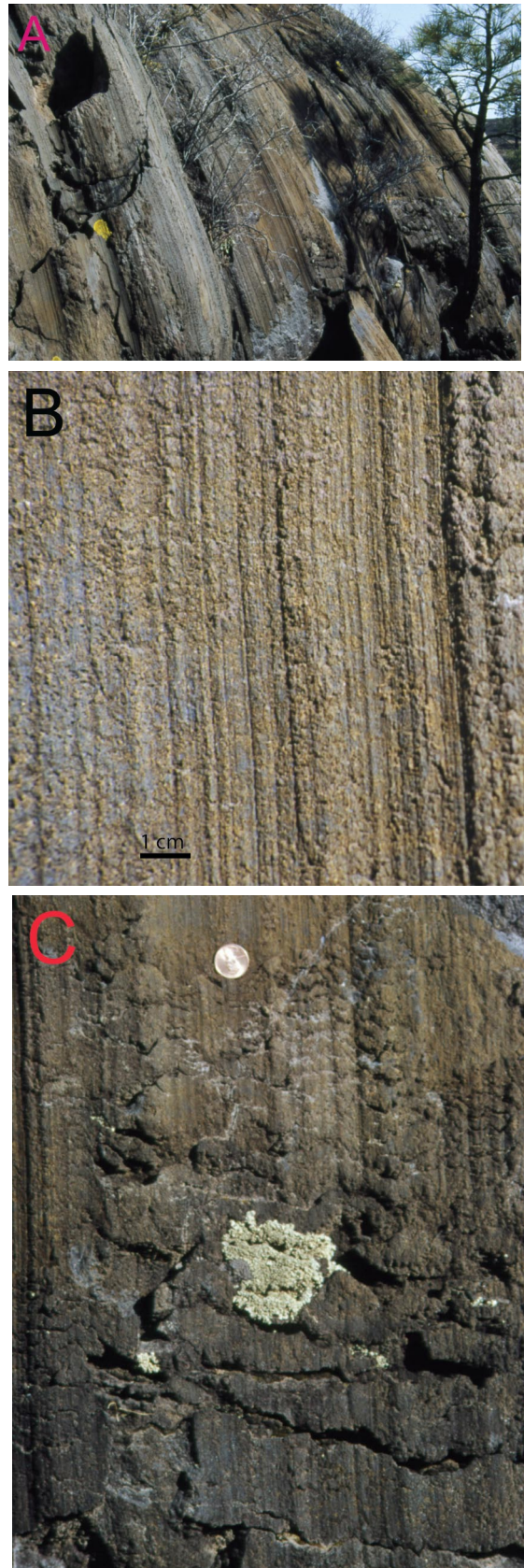


Figure 2. Lava squeeze-up at the <2000-year-old Bonito Flow, Sunset Crater, San Francisco volcanic field, northern Arizona, USA. (A) West side of two-sided, wedge-shaped squeeze-up. (B) Detail of striations on side of squeeze-up. (C) Fractured and disaggregated squeeze-up exterior.

erupted basalt (Chadwick et al., 1999). Parallel sets of lineations are up to tens of meters long with individual-groove relief of typically <5 cm. Grooves are smooth and glassy, with fine sediment accumulated in the grooves that accentuates visibility (Fig. 3A). Chadwick et al. (1999) interpreted the lineated glassy surfaces to have formed when a submarine lava lake drained from beneath a crust and the lineations were created “by the raking of molten lava by a solid overlying crust” as the lava emerged laterally from beneath the crust (Chadwick et al., 1999, p. 202). The newly formed and lineated crust itself is locally broken and marked by younger sets of lineations, presumably formed by the same mechanism (Fig. 3B).

Perhaps the most visually striking example of grooved lava is the corrugated fine-grained diorite at the Inca fortress of Sacsayhuamán in Cuzco, Perú (Figs. 4A, B). An approximately 100-m-wide outcrop of hypabyssal diorite is covered with a single set of grooves as much as a meter deep. The smallest striations, as little as one mm wide, are up to 20 m long (Feininger, 1978). The striated surface is hard, smooth, and resistant to weathering, and resembles slickenside lineations on silicified fault surfaces (e.g., Gabelman, 1967). The striated exterior of the outcrop is locally buckled and broken, but the interior remains unbroken as if only the striated exterior had become brittle at the time of buckling (Fig. 5A in Feininger, 1978). Grooves appear to project beneath adjacent limestone (Marocco, 1980; Ericksen, 1986), and both limestone and dioritic fragments “could be pried from the grooved surface of the diorite, the grooves on the slab undersides fitting into those on the diorite surface” (Ericksen, 1986). There seems little doubt that the striations were produced when the diorite was in a plastic state, and most observers have inferred that grooves were produced by abrasion of the hot, soft diorite against wall-rock irregularities during exhumation of the diorite, followed by hardening (Gabelman, 1967; Marocco, 1980; Ericksen, 1986).

Extrusion of dacite and rhyolite occasionally produces large striated edifices. For example, several months after the devastating 1902 eruption of the Caribbean volcano Mount Pelée, a spire was extruded upward from the volcanic summit, sometimes by more than 10 meters per day, reaching a height of ~300 m before collapse in early 1903 (Hovey, 1903). Gilbert (1904) estimated, based on the observations of others, that a total of about one kilometer of spire was extruded, but it fragmented and disintegrated almost as fast as it was extruded. The planar northeast face of the spire was marked by vertical grooves, inferred at the time as the product of “friction against the side of the conduit” (Hovey, 1903).

Volcanic activity at Mount St. Helens in Washington (USA) in 2004-2005 resulted in the near steady-state extrusion of a dacite plug at rates of one to several meters per day. The dacite extrusion was characterized by a lineated exterior reflecting irregularities in the extruding orifice (Figs. 5A, B, C; Iverson et al., 2006). Rock recovered from the striated exterior, although strong enough to maintain striated form, was described by Iverson et al. (2006) as “fault gouge” that

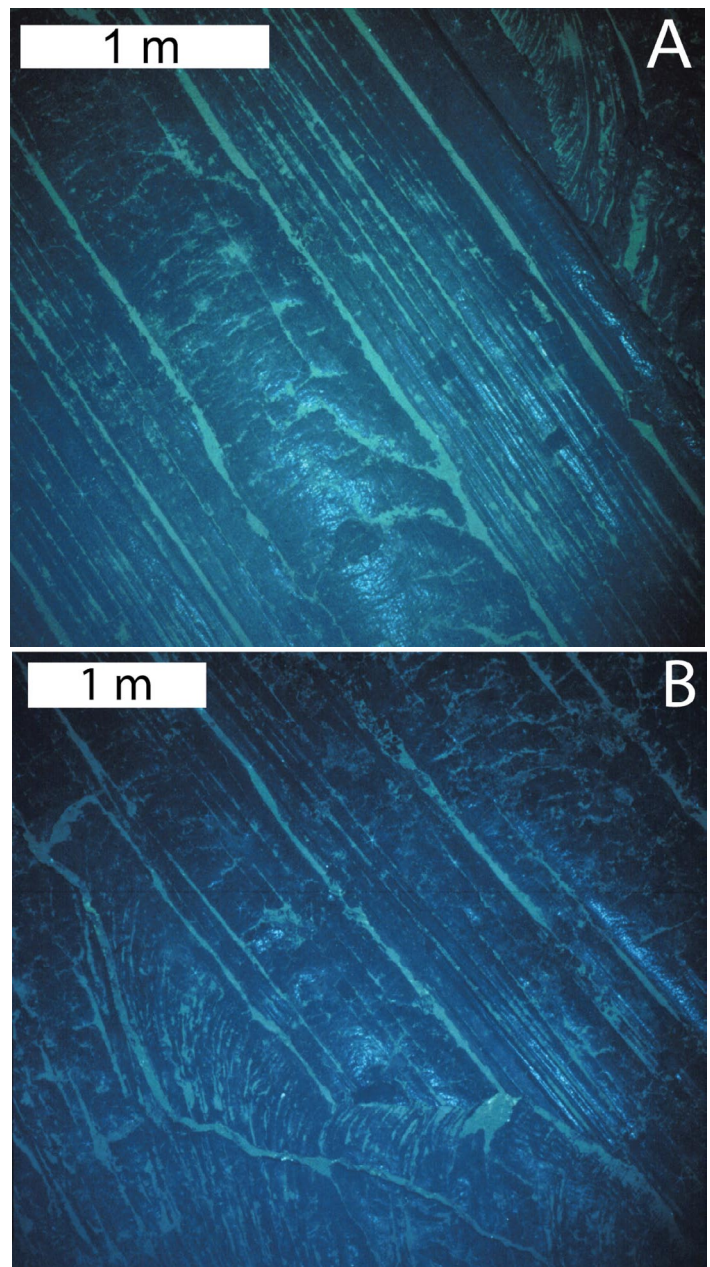


Figure 3. Lineated basalt-flow tops at the Young Sheet Flow (~2270 m water depth) on Juan de Fuca Ridge in the northeast Pacific (Chadwick et al., 1999). Photographs provided by Bill Chadwick, Oregon State University.

deformed largely or entirely by brittle processes. Extrusion was accompanied by periodic microseismicity within 1 km below the extrusion, with a recurrence interval of 30 to 300 seconds over more than a year. Striations at both Mount Pelée and St. Helens appear to have formed where a shallow magma chamber extruded its viscous contents upward into a confining orifice. Regardless of whether brittle or plastic shearing produced striations, the magma must have flowed upward into the confining orifice where it hardened as it was shaped and striated by the bounding solid rock.



Figure 4. Corrugated fine-grained hypabyssal diorite at the Inca fortress of Sacsayhuamán in Cuzco, Perú (photographs by Roland Brady, California State University, Fresno).

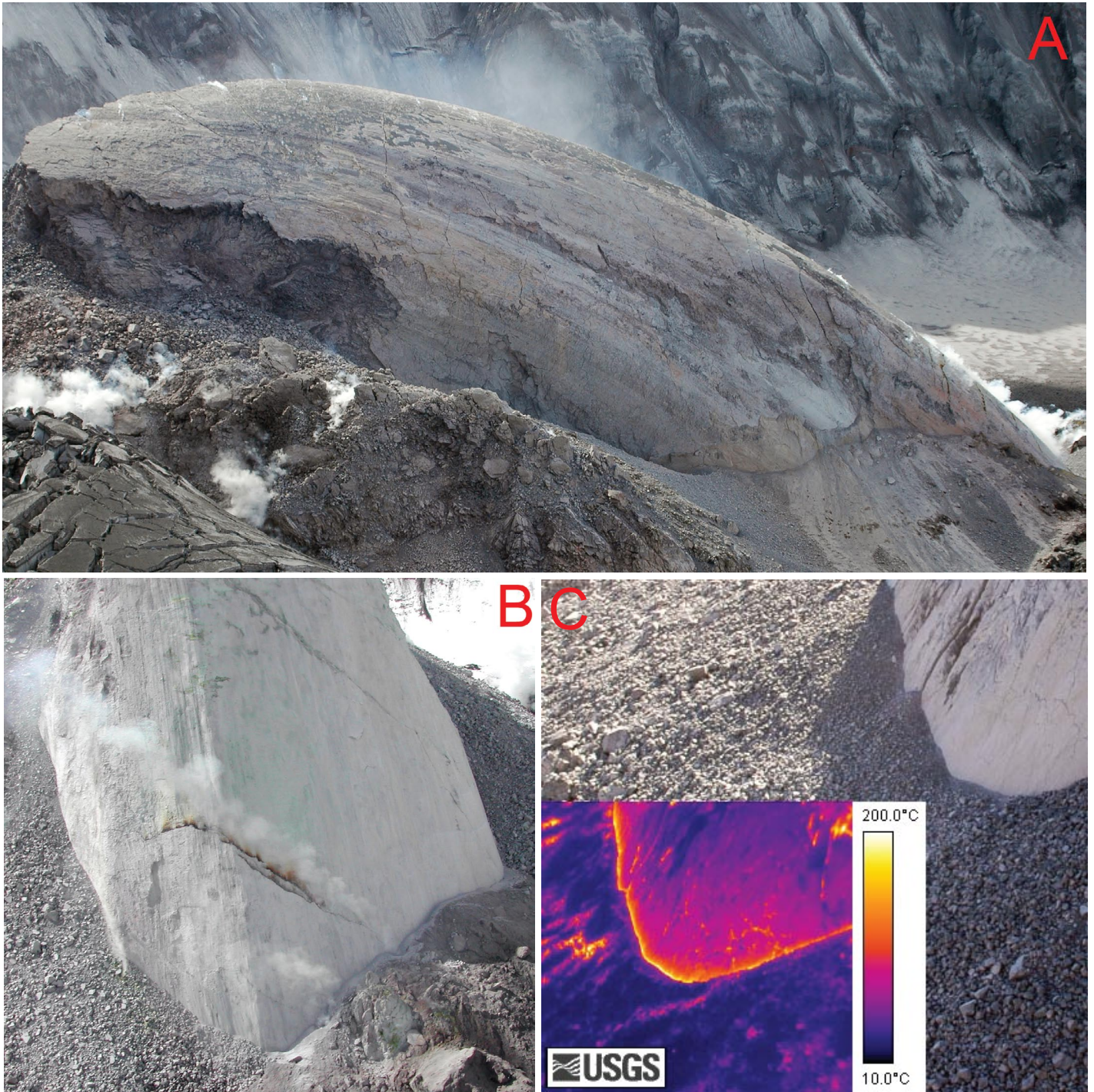


Figure 5. The dacite “whaleback spine” that was extruded in the crater of Mount St. Helens, Washington state, USA (Iverson et al., 2006). (A) Whaleback dacite extruded from right to left, striated by the molding orifice from which it emerged. Length of whaleback is ~380 meters. (USGS photograph taken on March 15, 2005, by Jim Vallance). (B) Base of whaleback extrusion and locus of emergence of extrusion (USGS photograph taken from the north on June 9, 2005 by Ken McGee). (C) Base of whaleback extrusion and locus of emergence of extrusion with infrared photograph showing temperature of extrusion and adjacent talus (USGS photographs taken on August 10, 2005 by Cynthia Gardner and Matt Logan).

TECTONIC CONTINUOUS CASTING

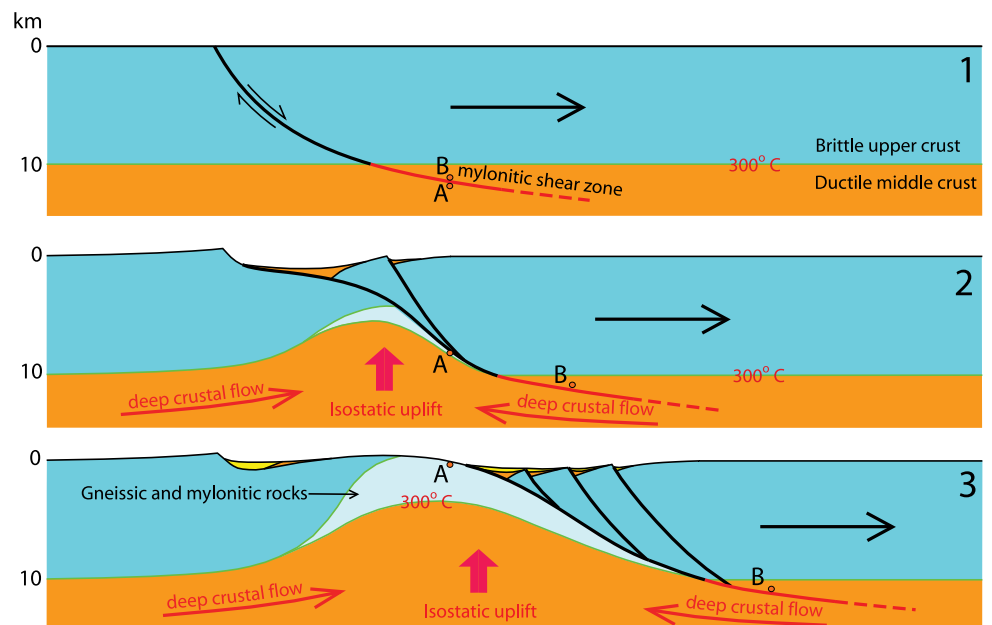
Metamorphic core complexes are areas of tectonic denudation where exhumed rocks were displaced from sufficient depth and temperature to have been affected by syn-exhumation mylonitic deformation and retrograde metamorphism (e.g., Davis et al., 1986; Fig. 6). Exhumation of each core complex was accommodated by large displacement on a bounding normal fault and occurred during lithospheric extension (e.g., Davis and Lister, 1987; Wernicke, 1992). Bounding normal faults are commonly moderately to gently dipping and known as “detachment faults”, especially where greenish, chloritically altered, brecciated footwall rocks are juxtaposed with hanging-wall rocks unaffected by similar alteration. Detachment faults are commonly grooved, with grooves parallel to extension direction and reflected in the form of the core complex if not deeply eroded. Originally identified in western North America (Crittenden et al., 1980), core complexes are now known on most continents, on the deep-sea floor, and possibly on Venus. Identification of remotely sensed core complexes is based on geomorphology, with grooved or domal form bounded on at least one side by a plausible normal fault, and on association with an extensional tectonic setting (e.g., Spencer, 2001).

High-angle faults are characterized by irregularities that would appear as grooves if fault displacement were sufficiently large and the footwalls tilted to gentle dips (Jackson and White, 1989). However, where grooves are tens of kilometers long, as in some complexes, either the fault and its down-dip continuation as a mid-crustal mylonitic shear zone formed simultaneously with a grooved form, or the most deeply exhumed rocks were molded into grooves as they flowed lat-

erally and upward into contact with the colder and stronger, grooved underside of the hanging-wall block (Fig. 7). In the former option, it remains unexplained why grooved mylonitic shear zones would develop with identical form to a brittle fault tens of kilometers up dip. Continuity of corrugated form through the low-strength environment of crystal-plastic flow is especially problematic where pluton-sized magma bodies are present because magma will flow in response to pressure differences without developing shear zones. Alternatively, core-complex footwalls could be derived from a middle crustal reservoir of plastically deforming or even molten rock that flows laterally and upward to be accreted to the trailing end of the fault footwall block and molded to the form of the hanging wall. This is the process of tectonic continuous casting (Spencer, 1999).

Tectonic continuous casting has been supported only by deductive reasoning about the origin of long grooves rather than by specific geologic features that require footwall molding to hanging-wall irregularities. One prediction of tectonic continuous casting is that footwall rocks should have flowed into antiformal grooves and out from beneath synformal grooves, imparting a slight to significant deviation from strict flow-path parallelism. Mylonitic lineations, if recording such flow, should converge regionally updip towards antiformal axes and diverge away from synform axes. A study specifically directed at identifying such lineation patterns at the west end of Tanque Verde Ridge in the Rincon Mountains east of Tucson, Arizona (USA) did not identify evidence for predicted convergent flow toward the antiformal axis (Perry, 2005). These results indicate that, if tectonic continuous casting occurred in such settings, it likely occurred during high temperature, low stress flow that preceded most or all development of mylonitic lineations.

Figure 6. Hypothetical three-stage cross-section evolution of core-complex genesis and exhumation. (A) Initial listric normal fault passes downward into a gently dipping mylonitic shear zone which dies out laterally and downward into the weak and mobile middle crust. (B) Tectonic denudation of the fault footwall, due to crustal extension, results in isostatic uplift and arching of the footwall. Deep mobile crust flows in response to lateral pressure gradients which result from decreased overburden above the denuded fault (e.g., Block and Royden, 1990; Wernicke, 1992). (C) Gneissic and mylonitic rocks that had resided in the plastic middle crust at the time that faulting began, or at least in the transition downward into the crystal-plastic deformation regime, are completely exhumed and become a source of mylonitic and gneissic debris shed into syn-tectonic hanging-wall basins.



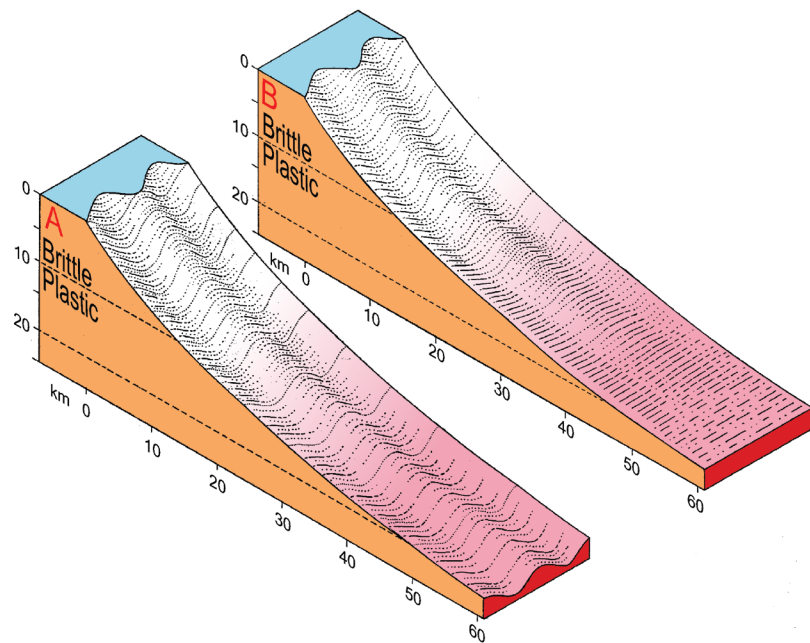


Figure 7. Block diagram of alternative geometries for initial detachment-fault footwall corrugations (from Spencer, 1999). Corrugated fault footwall extends downward and laterally into the weak, ductile middle crust where it becomes a mylonitic shear zone and (A) maintains corrugated form for indefinite lateral distance, or (B) grades into a planar shear zone. There is no mechanical rationale for simultaneous development of a corrugated shear zone over indefinite lateral distance, so (B) is considered more likely. However, continuous casting does not require any particular shear-zone geometry, only that the weak or even magmatic middle crust flow laterally and/or upward into contact with a colder and stronger, corrugated hanging wall.

Deep-sea metamorphic core complexes

Plate divergence leading to generation of new oceanic lithosphere is accompanied by voluminous basaltic magmatism at high spreading rates, but at moderate to slow spreading rates, magmatism is at least intermittently suppressed. Sea floor produced by moderate spreading rates is locally characterized by grooved, gently sloping surfaces that are commonly hundreds of square kilometers in extent, with grooves parallel to spreading direction and to nearby transform faults (e.g., Cann et al., 1997; Tucholke et al., 1998; Blackman et al., 1998; Christie et al., 1998; Ohara et al., 2001; Okino et al., 2004; Drolia and DeMets, 2005). Dredge samples from grooved surfaces include mylonitic peridotite, serpentinite, cataclasite, and various mafic and ultramafic rocks that have been deformed, metamorphosed, and hydrothermally altered (e.g., Karson and Dick, 1983; Cannat et al., 1991; Cannat, 1993; Jaroslow et al., 1996; Cann et al., 1997; Dick et al., 2000; Harigane et al., 2008). The grooved surfaces have been interpreted as metamorphic core complexes that were exhumed during asymmetric lithosphere spreading with somewhat suppressed magmatism. Multibeam-sonar bathymetric mapping has imaged dozens of grooved complexes, but has surveyed only a tiny fraction of the sea floor. It is likely that there are more core complexes in the deep sea than on land.

Deep-sea core-complex grooves have been termed “mullions” or “megamullions” in relevant literature (e.g., Tucholke et al., 1998; Ohara et al., 2001, 2003a, b). The Glossary of Geology (Neuendorf et al., eds., 2005, 5th ed.) defines “mullion” as “A type of lineation in metamorphic rock formed where the interface between lithologies with differing ductilities becomes corrugated...”. Although the fifth edition of the Glossary of Geology does not mention slip surfaces or faults in the context of “mullions,” the second edition states that

“Mullions may be formed parallel to the direction of movement, as along fault planes...” (Bates and Jackson, eds., 1980). The terms “mullion” and “megamullion” have been applied to oceanic but not continental metamorphic core complexes, but this should not be taken to indicate that they are formed by fundamentally different processes. In this regard, “mullion” and “megamullion” are synonymous with “groove” and “corrugation” and do not imply a specific formative process.

Godzilla Mullion, Philippine Sea. The longest known tectonic grooves on Earth are present at the Godzilla Mullion in the Parece Vela Basin of the Philippine Sea (Fig. 8; Ohara et al., 2001, 2003a, b; Harigane et al., 2008). The grooved complex is 125 km long and up to 55 km wide (~6000–7000 km²; larger than the U.S. State of Delaware), with individual grooves as long as 60 km. An adjacent transform fault parallels the grooves, whereas abundant abyssal hills and the adjacent extinct spreading center are perpendicular to the grooves, as with other deep-sea core complexes. The large, 60-km-long antiformal groove in the southern part of the complex is ~5 km wide. An ~0.7-km-wide synformal groove along the southern part of its crest reveals the smallest discernable groove wavelength. The Godzilla grooves change trend by ~7° along the length of the complex and parallel the curving strike of the adjacent transform fault and other transform faults along the extinct Parece Vela Rift (Fig. 8; Kasuga and Ohara, 1997; Okino et al., 1998; Ohara et al., 2001).

The grooved complex was interpreted by Ohara et al. (2001) as the footwall of a normal fault beneath which 125 km of sea floor was created by extension along the Parece Vela Rift, which has been extinct since ~12 Ma (Okino et al., 1998; Ohara et al., 2003a, b). This interpretation is supported by analysis of dredge samples. Petrologic analysis of dredged gabbro from near the presumed detachment breakaway at the southern end of the Godzilla Mullion reveals evidence of

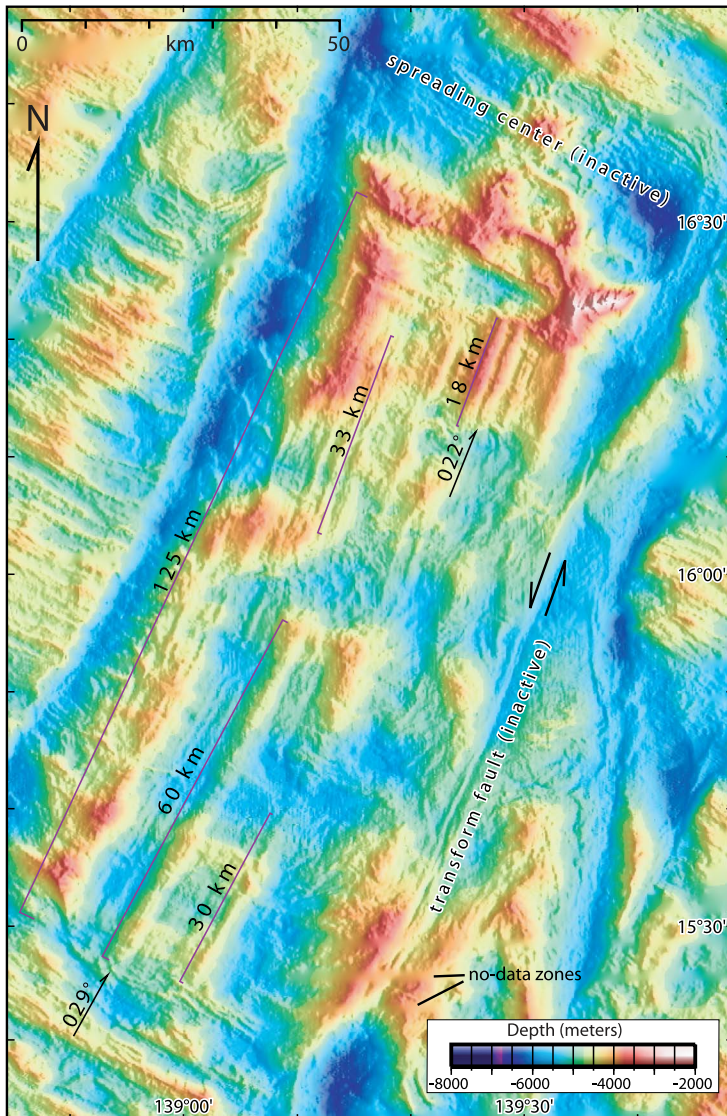


Figure 8. Godzilla Mullion in the Parece Vela Basin of the Philippine Sea. Multibeam bathymetry data were acquired by the Hydrographic Department of Japan aboard survey vessel Takuyo in 1995-1997 (details of data acquisition are provided by Okino et al., 1998).

crystal plastic deformation, including undulose extinction, deformation twinning, subgrain development, and crystal preferred orientation in plagioclase and clinopyroxene (Harigane et al., 2008). Retrograde metamorphism during deformation produced sodic plagioclase and hornblende (Harigane et al., 2008). Recovery of fertile peridotite from the Godzilla Mullion is consistent with the inference that deep-sea core complexes reflect a tectonic setting of reduced magmatism (Ohara et al., 2003a; Snow et al., 2004). However, recent dredging on the mullion yielded significant amount of gabbroic rocks (Ohara et al., 2007), which is consistent with the recent proposal that a long-lived detachment fault requires neither too low nor too high magmatism, but instead an intermediate amount (Tucholke et al., 2008).

Strong parallelism between grooves, and between grooves and adjacent transform faults, is consistent with an origin by continuous casting in which groove trend records plate divergence even as divergence direction changed. The changing groove trend along groove axes is analogous to the curving trend of grooves on lava blocks at McCartys flow where the slip vector between mold and lava changed during casting (Fig. 3 in Nichols, 1938). However, there is great uncertainty as to whether the plasticity of footwall rocks that were molded into grooves was due to high temperatures and intermittent magmatism (Tucholke et al., 2008), to serpentinized peridotite that behaves plastically at moderate to low temperatures (e.g., Spencer, 2003), or to other factors. The grooves are so well developed, and the molding behavior apparently so consistent over long groove lengths, that consistent rheology during extrusion seems to be required.

Continental metamorphic core complexes

Wasatch fault, Utah, western USA. Part of the Wasatch fault system is discussed here because it represents an active and well studied area of normal faulting and fault corrugations. Fault displacements are not sufficient to uncover mylonitic mid-crustal rocks, but parts of the system appear to be close to the transition where such rocks are exhumed and so may be instructive about core-complex groove genesis. The moderate dips of parts of the fault system are also suggestive of an underway transition to low-angle detachment faulting.

Active continental normal faults are typically characterized by topographic embayments and promontories that reflect the form of the normal fault and its uplifted footwall. Segmentation is common in young normal-fault systems where fault segments have not yet connected and fault tips are separated by relay ramps. With greater displacement, fault segments connect either by propagation of curved fault tips or development of new, linking faults (Ferrill et al., 1999). The ~350-km-long Plio-Quaternary Wasatch fault zone, at the eastern boundary of the northern Basin and Range province in the western United States, is one of the best mapped and studied active normal-fault zones. It consists of ten structural segments, each separated from adjacent segments by fault-zone irregularities such as relay ramps and footwall promontories. Each segment appears to have ruptured independently during the Holocene (“earthquake segments” of Machette et al., 1991) but similar long-term displacement rates suggest linkage over millions of years (Armstrong et al., 2004). With sufficient displacement and footwall tilting, the promontories and embayments will become gently plunging corrugations.

Oligocene granite of the Little Cottonwood stock forms perhaps the largest promontory in the footwall of

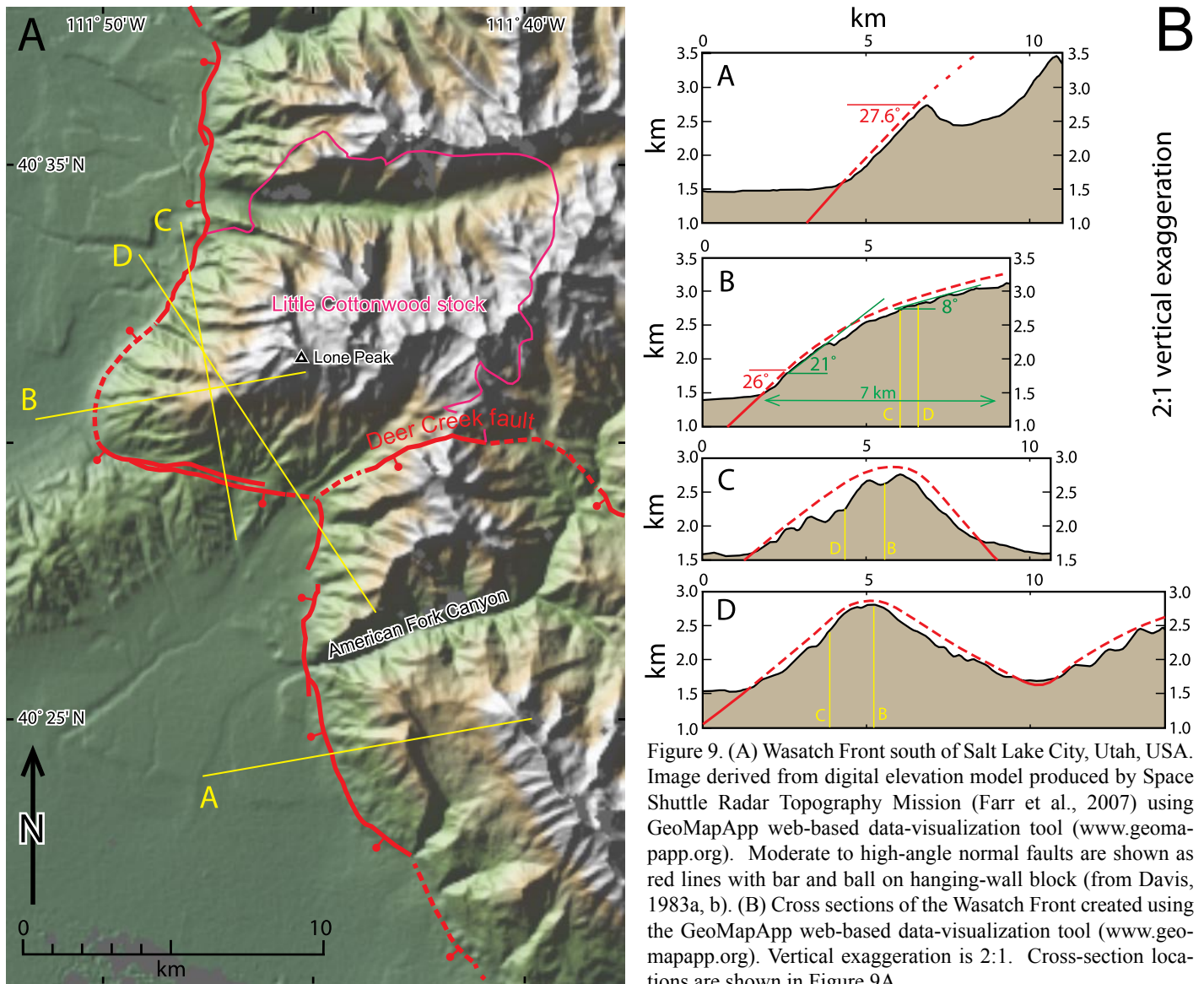


Figure 9. (A) Wasatch Front south of Salt Lake City, Utah, USA. Image derived from digital elevation model produced by Space Shuttle Radar Topography Mission (Farr et al., 2007) using GeoMapApp web-based data-visualization tool (www.geomapapp.org). Moderate to high-angle normal faults are shown as red lines with bar and ball on hanging-wall block (from Davis, 1983a, b). (B) Cross sections of the Wasatch Front created using the GeoMapApp web-based data-visualization tool (www.geomapapp.org). Vertical exaggeration is 2:1. Cross-section locations are shown in Figure 9A.

the Wasatch fault zone (Fig. 9; Lone Peak salient of Gilbert (1928)). The east-west striking, south-dipping segment of the Wasatch fault on the south side of the stock is approximately aligned with the Deer Creek fault in the footwall of the Wasatch fault. The Wasatch fault west of the intersection could have accommodated the combined displacements of the Wasatch fault to the south and the Deer Creek fault to the east (Bruhn et al., 1987), but the minor to non-existent geomorphic signature of Deer Creek fault indicates that it contributed little Plio-Quaternary displacement. However, its alignment with the south-dipping segment of the Wasatch fault suggests that it was reactivated and/or utilized by the Wasatch fault. Fluid-inclusions from fault rocks along the Wasatch fault where it cuts Little Cottonwood stock indicate fluid pressures during faulting that correspond to paleodepths of at least 11 km (Parry and Bruhn, 1987). Such paleodepths are difficult to reconcile with the approximately 2 km of relief along the Wasatch range

front and assertions that the “Wasatch fault zone consists of 45°-60° dipping normal faults...” (Armstrong et al., 2004).

Large paleodepths of exposed Wasatch footwall rocks can be readily reconciled with modest range-front relief if the Wasatch fault is convex upward and steep only at depth, and if exhumation resulted in deformation of the footwall so that it flexed and flattened in response to isostatic unloading (rolling-hinge model of Wernicke and Axen (1988) and Buck (1988)). In contrast to the statement above by Armstrong et al. (2004), Gilbert (1928) identified five locations where fault dips are 29° to 35°, another where dip is 33° to 37°, and another where it is 35° to 45°. The planar geomorphic surface that forms the slightly eroded footwall of the Wasatch fault south of American Fork Canyon dips 27° to 28° over a vertical range of 1200 meters (cross-section A in Figure 9). Gilbert (1928, p. 22) also identified the convex-upward nature of the Wasatch fault footwall at Lone Peak salient (equivalent to the

promontory at Little Cottonwood stock), stating the following about the feature represented in cross-sections B, C, and D in Figure 9:

“The measurement at Fort Canyon, 29°, was on the southern face of the salient, and that near Draper, 35°, on the western face. Between the two places lies the rounded apex of the salient, and the dips diminish toward the apex where the angle indicated by the rock profile is 20°. Traces of fault friction were not observed at the apex, but there is much evidence that the original form of the granite body is well represented by the present contours and profiles near the rock base. From the apex of the salient to the high crest in the direction of Lone Peak the granite presents a blunt edge that separates the southerly and westerly faces. Those faces are relatively steep, but the profile of the edge itself is gentle. It is also convexly curved, from 10° in its higher part to 20° at the rock base....If the local profile of the granite should be explored below the surface, it would probably be found to steepen.”

Note that Gilbert did not think that the convex form of the Lone Peak salient resulted from footwall flexure, rather that “the unyielding granite prong plowed a furrow through the weaker rocks of the hanging wall” (Gilbert, 1928, p. 22).

The Lone Peak salient is an exhumed corrugation of the Wasatch fault that is perhaps larger in amplitude than any core complex corrugation. It is not yet a metamorphic core complex, however, because mylonitic fabrics produced down-dip from the Wasatch fault have not yet been exhumed. The Lone Peak salient is the exhumed conjugate to a hanging-wall furrow that, with greater fault displacement, would potentially become the mold for a large, exhumed, antiformal cast groove. We emphasize that there is no evidence that the salient was shaped by continuous casting, but rather that it formed a strong granite-footwall prong that possibly deformed the hanging wall, as interpreted by Gilbert (1928).

Dayman dome, Owen Stanley Range, Papua New Guinea. Dayman dome of the Suckling-Dayman massif in eastern Papua New Guinea is one of the very few active continental metamorphic core complexes. Metamorphic grade in the complex, which consists primarily of Late Cretaceous basalt and limestone, increases from prehnite-pumpellyite in the south to pumpellyite-actinolite in the north, indicating increasingly high-pressure metamorphism in more northerly exposures (Davies, 1980). A low-angle fault at the margins of the dome is associated with greenschist-facies metamorphism and a strong tectonite fabric that is also domed (Davies, 1980). At least part of the tectonite fabric is a mylonitic shear zone with top-north-northeast normal displacement (Daczko et al., 2007).

The low-angle fault that bounds the northern and eastern margins of the dome is clearly apparent in aerial photographs and in topography (Fig. 10; Davies, 1980; Ollier and Pain, 1980, 1981). The remarkable smoothness of the footwall at the foot of the dome was interpreted to indicate that the bounding

normal fault is active and that the freshly denuded footwall has not yet been extensively or deeply incised in spite of abundant tropical rainfall (Ollier and Pain, 1980, 1981). The 18° to 23° north dip of the surface at the foot of the dome is interpreted as the dip of the bounding normal fault (cross-sections A-D in Figure 10). The dome is broadly arched, with an incised but locally planar south-dipping surface on the south side of the dome (Davies, 1980; Ollier and Pain, 1981; cross-sections A and B in Figure 10). The lateral extent of the denuded footwall in the direction of extension is at least 20 kilometers (cross-section C in Figure 10), which represents the minimum fault displacement and extension magnitude. Association of an arched, top-north, large-displacement, low-angle normal fault with a mylonitic shear zone with top-north sense of shear indicates that the Dayman dome is a metamorphic core complex. Furthermore, it forms the west end of a belt of metamorphic core complexes exposed in the D’Entrecasteaux Islands to the east (Hill et al., 1992; Baldwin et al., 2004; Little et al., 2007; Webb et al., 2008). The entire belt of extension is located west of the propagating tip of the Woodlark spreading center (Martínez et al., 1999).

Although the domal form of Dayman dome has been emphasized in previous studies, the dome is also grooved. The plunging axis of an antiform forms a range-front promontory at the north foot of the dome, three kilometers east of cross-section C in Figure 10. An embayment in the range front reflects the form of a plunging synformal groove (cross-section A in Figure 10 is located on the synform axis). Both of these features, as well as more subtle grooves, are visible in cross-sections E and F (Fig. 10). The west side of the largest antiformal groove forms a smooth, sloping surface directly west of the summit of Mount Dayman (cross-section G in Figure 10). The west flank of the groove is a topographic feature over ~20 km parallel to extension direction. These grooves reflect the form of the bounding normal, as with other normal faults such as along the Wasatch front.

Abundant linear drainages mostly trend down slope, but some are rather oddly positioned. One drainage trends down the axis of the largest antiform rather than descending down either flank (red-arrow “1” in Figure 10 points toward this drainage). A linear drainage approximately one kilometer east of this drainage, even though located slightly down the east flank of the antiform, parallels the antiform axis (drainage 2), as does another farther down the flank (drainage 3). Two other parallel drainages (drainages 4 and 5) might be expected to converge down-plunge because they both occupy a synform, as revealed in cross-section E and by the trace of the range-foot normal fault. However, the western groove (drainage 4) remains slightly up the western side of the synformal groove where it receives and deflects water from small drainages that flow northeastward down the flank of the large antiform. All of these groove-parallel drainages trend ~019°. We interpret these drainages to have formed in tectonic grooves of the fault surface that are too small to be visible in the fault trace at the foot of the dome. It is also possible that drainages

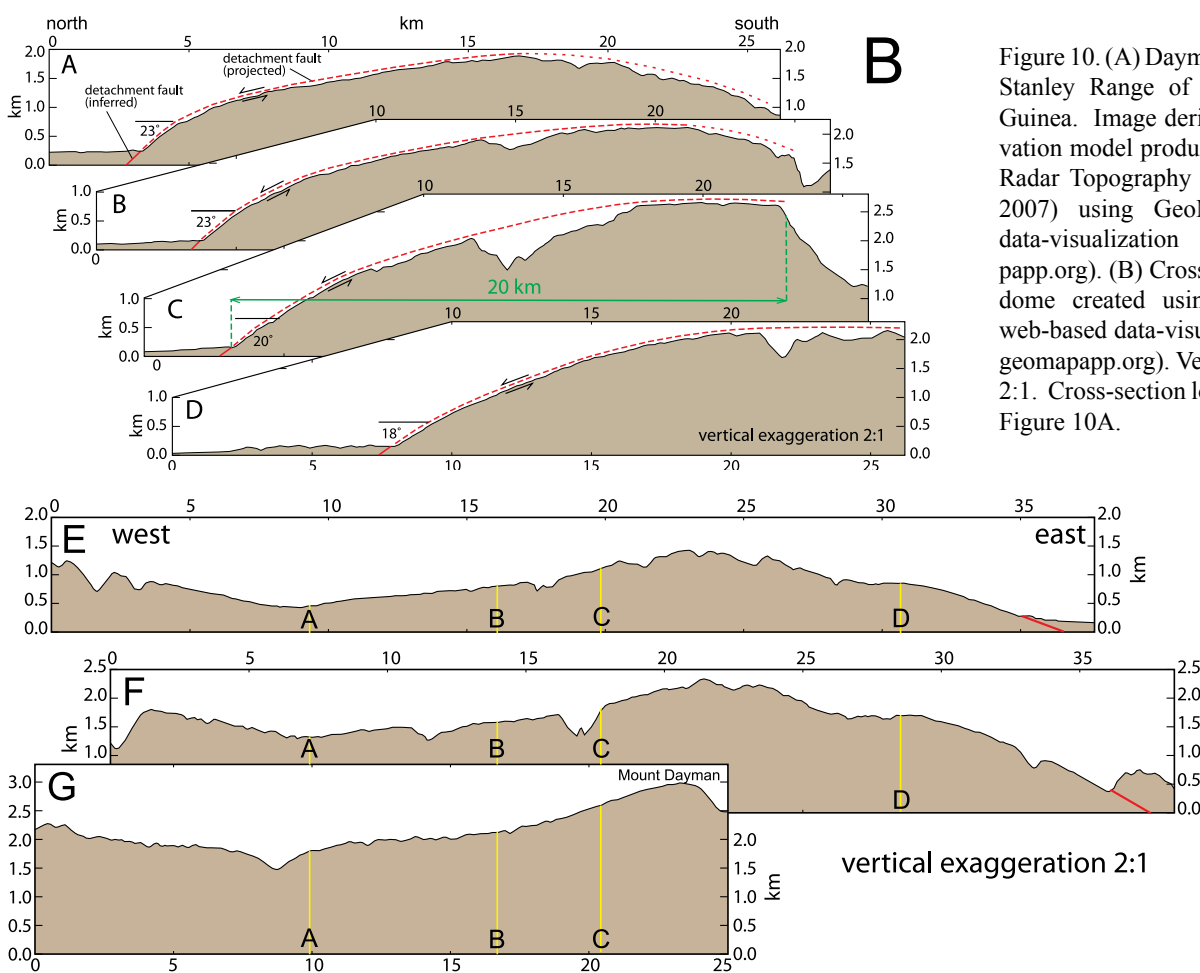
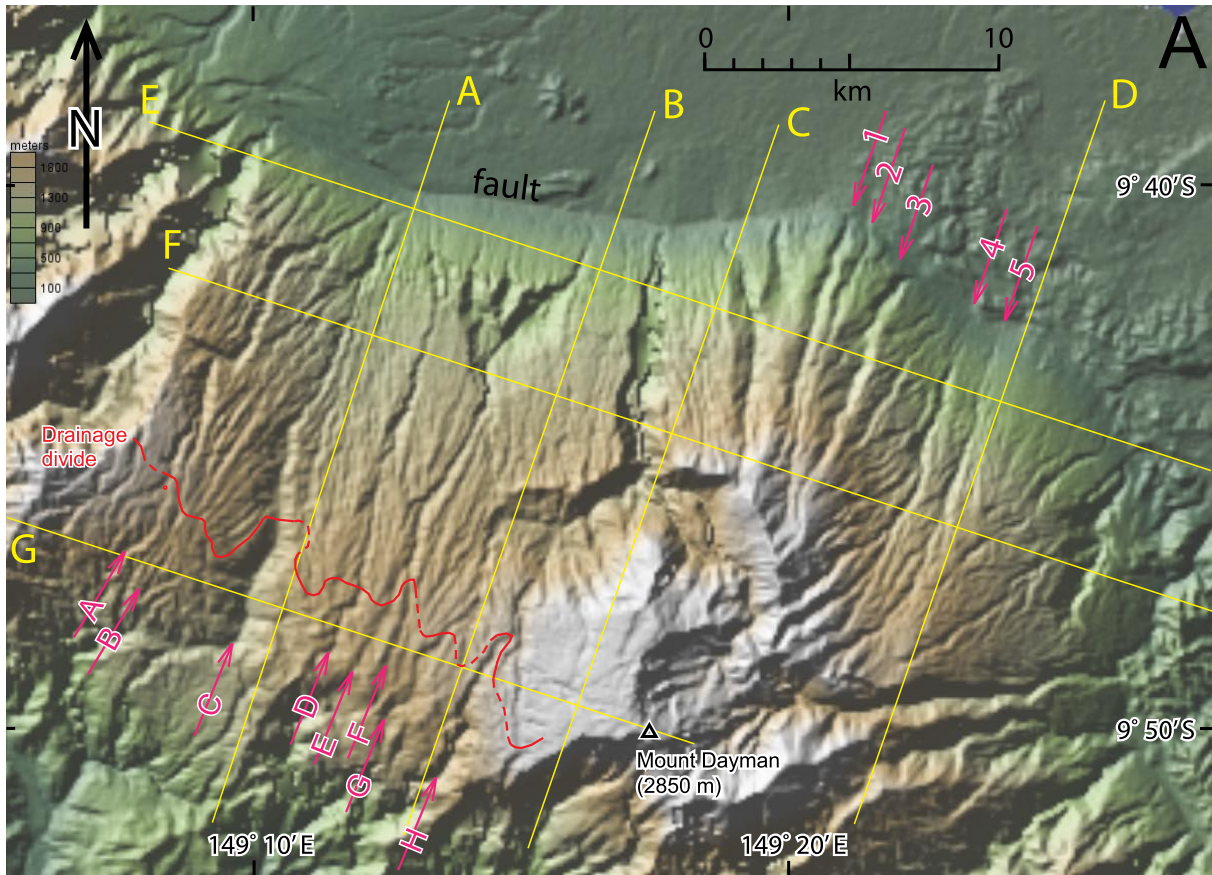


Figure 10. (A) Dayman dome in the Owen Stanley Range of eastern Papua New Guinea. Image derived from digital elevation model produced by Space Shuttle Radar Topography Mission (Farr et al., 2007) using GeoMapApp web-based data-visualization tool (www.geomapp.org). (B) Cross sections of Dayman dome created using the GeoMapApp web-based data-visualization tool (www.geomapp.org). Vertical exaggeration is 2:1. Cross-section locations are shown in Figure 10A.

in the hanging-wall block guided elongating drainages down the freshly denuded footwall surface with each increment of fault displacement. This second alternative is favored by the association of these drainages with incised topography in the hanging-wall block of the fault, unlike areas farther west. In either case, and if correctly interpreted, these drainages reveal the displacement direction of the bounding fault (Spencer, 2000), as do the map-scale grooves.

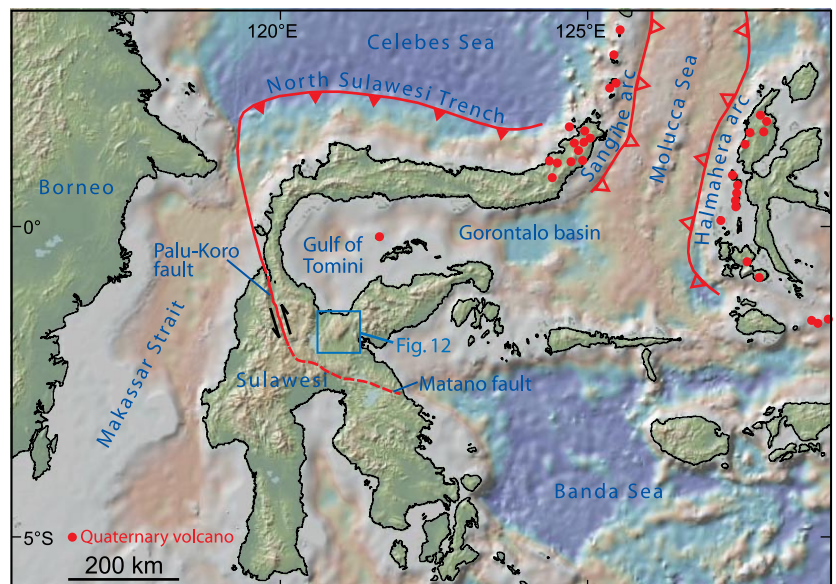
Cross sections of the dome oriented parallel to extension clearly show the arched form of the footwall, with increasing radius of curvature away from the active fault trace. The southward-increasing radius of curvature is most readily interpreted as unbending of the curved footwall as it flattens after exhumation (Wernicke and Axen, 1988; Buck, 1988), reflecting the low flexural strength of footwall rocks exhumed from beneath detachment faults. Footwall pliability is presumably due to high temperatures associated with deep-crustal residence before tectonic exhumation. The simplest interpretation of the dome is that it is at a more advanced stage of extension than the Wasatch front, but is otherwise structurally similar. Low footwall-block strength, indicated by mylonitization and by unbending following denudation, are permissive of, but do not require, continuous casting of the northernmost ends of the grooves.

A remarkable and previously unappreciated aspect of Dayman dome is the continuity of drainages across the drainage divide at the crest of the range (red irregular line in Figure 10). Eight drainages on the south side of the arch are identified (red arrows and letters in Figure 10) that have counterparts on the north side. One is an ~1-km-wide canyon (arrow “C”). Arrow “B” points to a pair of parallel but subtle drainages, ~300 m apart, that are aligned with two discontinuous drainages with the same azimuth and spacing north of the arch crest. Drainage F forms a straight line with a drainage on the north side of the arch, but near the drainage divide appears

connected with a different, parallel drainage. Alignment of drainages in this manner is known at South Mountain, an early Miocene metamorphic core complex in Arizona (Reynolds, 1985). In both complexes, such drainages are readily interpreted as the result of back tilting due to isostatic uplift and arching of the core complex in response to tectonic denudation (Spencer, 1984, 2000). According to this interpretation, all south-flowing drainages at Dayman dome were originally north-flowing drainages. Barbed drainages would be expected for drainage reversal, and although not obvious on the south side of Dayman dome, one is present upstream from arrow “A” (at the small red dot in Figure 10 which represents the point where an east-northeast-flowing drainage is deflected to become a south-southwest-flowing drainage). An alternative interpretation of the aligned drainages is that they follow weak layers of rock, or pervasive fractures, that are steeply dipping and east-northeast striking. However, there are no apparent geomorphologic consequences of such layering or fabric in the walls of the deep canyons that incise the complex. Furthermore, except for those drainages that parallel the antiform axis in the northeastern part of Dayman dome, drainages seem to be oriented locally downslope, converging toward synform axes and diverging from antiform axes.

Central Sulawesi, Indonesia. The very active tectonics of eastern Indonesia result from its position at a triple junction between the Pacific, Indo-Australian, and Eurasian plates. In detail, the triple junction is marked by multiple small plates and convergent margins, including arc-arc collision in the Molucca Sea northeast of Sulawesi and westward displacement of a fragment of western New Guinea (Irian Jaya) into eastern Sulawesi (Hamilton, 1979; Hall, 2002, 2008). The 600-km-long, east-west-trending North Sulawesi trench, north of the northern arm of Sulawesi, accommodates northward displacement of northern Sulawesi over the Celebes sea floor (Fig. 11; Silver et al., 1983). The Gulf of Tomini and Gorontalo

Figure 11. Map of Sulawesi and surrounding area showing location of Figure 12. The image was derived from a digital elevation model produced by the Space Shuttle Radar Topography Mission for land areas (Farr et al., 2007) and a global bathymetric data set derived from satellite altimetry and ship depth soundings for ocean areas (Smith and Sandwell, 1979). The image was prepared using GeoMapApp web-based data-visualization tool (www.geomapapp.org) with volcanoes from Hamilton (1979, Plate 1) and coastlines from Hall (2008, Fig. 1). Red faults with solid teeth are subduction-zone thrusts, with hollow teeth are secondary back-thrusts following collision of two forarcs beneath Molucca Sea.



basins, which separate the north arm of Sulawesi from central Sulawesi, contain up to several kilometers of Neogene sediment (Hamilton, 1979). Complex and poorly understood late Cenozoic deformation in central Sulawesi is linked to the Palu-Koro left lateral fault in western Sulawesi and the Matano fault in central Sulawesi (Silver et al., 1983; Bellier et al., 2006; Socquet et al., 2006).

An ~2000 km², dome-like massif, south of the Gulf of Tomini and centered on the Pompangeo Mountains in central Sulawesi (Fig. 12A), is characterized by several geomorphic features similar to Dayman dome and other metamorphic core complexes. The surface of the dome slopes 4°-14° northwestward along its northwest flank to project beneath hills south of the city of Poso. The northeastern margin of the massif slopes ~10° northward beneath a narrow coastal plain (Fig. 12B, cross-sections B, C). The Pompangeo massif is broadly grooved, with a central groove that has an ~10-km-wide, plateau-like top with outward-sloping flanks (cross-sections D and E in Figure 12B). Two antiforms and flanking synforms are present between the high, central part of the massif and Lake Poso to the west. The massif is incised by abundant, corrugation-parallel drainages (Fig. 12A). Many drainages depart from the dominant, ~N17°W drainage trend, and instead plunge obliquely outward from antiform axes. Some of these drainages are intercepted by groove-parallel drainages (especially drainages just west of cross-section A in Figure 12A and drainages south of Uekuli). Highly linear drainages are aligned across drainage divides, some linear drainages are essentially horizontal at drainage divides, and one seems to contain a small closed basin. One linear drainage perched on the axis of the highest, central antiformal groove descends gently north-northwestward with a one-degree slope over 7 km (between arrows of cross-section line A in Figure 12A), unaffected by the steep westward slope of the antiform flank only 1 km to the west. Barbed drainages on the south side of the massif suggest that north- or northwest-flowing streams were captured by south- or southeast-flowing streams (Fig. 12A).

The Pompangeo Schist Complex, which underlies the Pompangeo Mountains and areas to the west around Lake Poso, consists largely of interlayered phyllitic marble, calcareous phyllite, graphitic schist, and quartzite, and in eastern exposures, tectonic mélange including serpentinite and metamorphosed mafic igneous rocks (Parkinson, 1998; Villeneuve et al., 2002). A “strong transposition foliation” strikes north-northwest and dips gently to moderately to the west-southwest, and “microstructural fabrics indicate a top-to-east sense of shear” (Parkinson, 1998). A stereonet presented by Parkinson (1998, Fig. 5) indicates that the average dip of transposition foliation (n=115) is 20°-30° west-southwest, although foliations plotted in Parkinson’s Figure 3 map appear steeper and more diversely oriented. L₁ stretching lineations and F₁ fold hinges are parallel to the dominant drainage set (Fig. 5 in Parkinson, 1998) and plausibly related to mylonitization in a core complex, but the spatial distribution of structural measurements is not clear. Parkinson (1998) also reported three

mid-Cretaceous K-Ar dates, two from “mica” and one from a whole-rock sample of metabasite, derived from rocks considered to be part of the metamorphic assemblage west of Lake Poso. Hamilton (1979, Fig. 86) attributed the linear tectonic grain of topography at the top of the Pompangeo Mountains to steep bedding and foliation, with oblique truncations of the abundant linear ridges due to “severe imbrication.” Parkinson (1998, Fig. 6), using what appears to be the same aerial photograph as presented by Hamilton, reiterated this interpretation by showing the traces of inferred imbricating thrusts. Both authors interpreted the abrupt westward termination of lineated topography in this photograph as due to “Neogene sedimentary rocks [that] cover the deformed complex” (Hamilton, 1979, p. 168; Poso Formation of Parkinson, 1998). It is clear from Figure 12A, however, that the termination of lineated topography is due to the abrupt drop off to the west where rapid erosion of the steep slope has destroyed the lineated topography.

The geomorphology of the massif resembles Dayman dome in Papua New Guinea in three characteristics: (1) domal morphology bounded on one side by a contact, readily interpreted as a low-angle normal fault, where the dome surface projects downdip beneath a region of completely different topographic character, (2) corrugated form of the domal massif, and (3) linear drainages parallel to corrugations. However, moderate dips of the transposition foliation of the Pompangeo Schist Complex may be responsible for much of the linear drainage geometry. In this case, the similarity to the Dayman Dome and other core complexes is coincidental. It may be that some of the linear drainages, especially in northern exposures, are related to tectonic exhumation from beneath a low-angle normal fault. The delicate, parallel drainages visible in Hamilton’s aerial photograph are geomorphically immature, with ongoing destruction where slopes are steeper. Plio-Quaternary exhumation of a smooth, gently sloping fault surface overlying steeply foliated schist would be ideal for creating such drainages, especially if foliation strikes parallel to the slope of the denuded fault footwall.

On the basis of similarity of Pompangeo massif geomorphology to the geomorphology of known metamorphic core complexes, we suggest that the Pompangeo Schist Complex is the denuded footwall of a large-displacement low-angle normal fault. Furthermore, if this interpretation is correct, then the large size of the Pompangeo Schist Complex suggests that at least its northern extent includes mylonitic fabrics related to exhumation, in which case part of the Schist Complex would be a metamorphic core complex. The very slight incision of the northern foot of the complex suggests that detachment faulting and exhumation are ongoing, and that much of the geomorphic expression of the complex is due to Plio-Quaternary tectonic exhumation. Furthermore, barbed drainages and drainages aligned across drainage divides suggest that the south flank of the massif has been tilted southward from an original northward slope. Many drainages appear to have been split in two by slope reversal of southern,

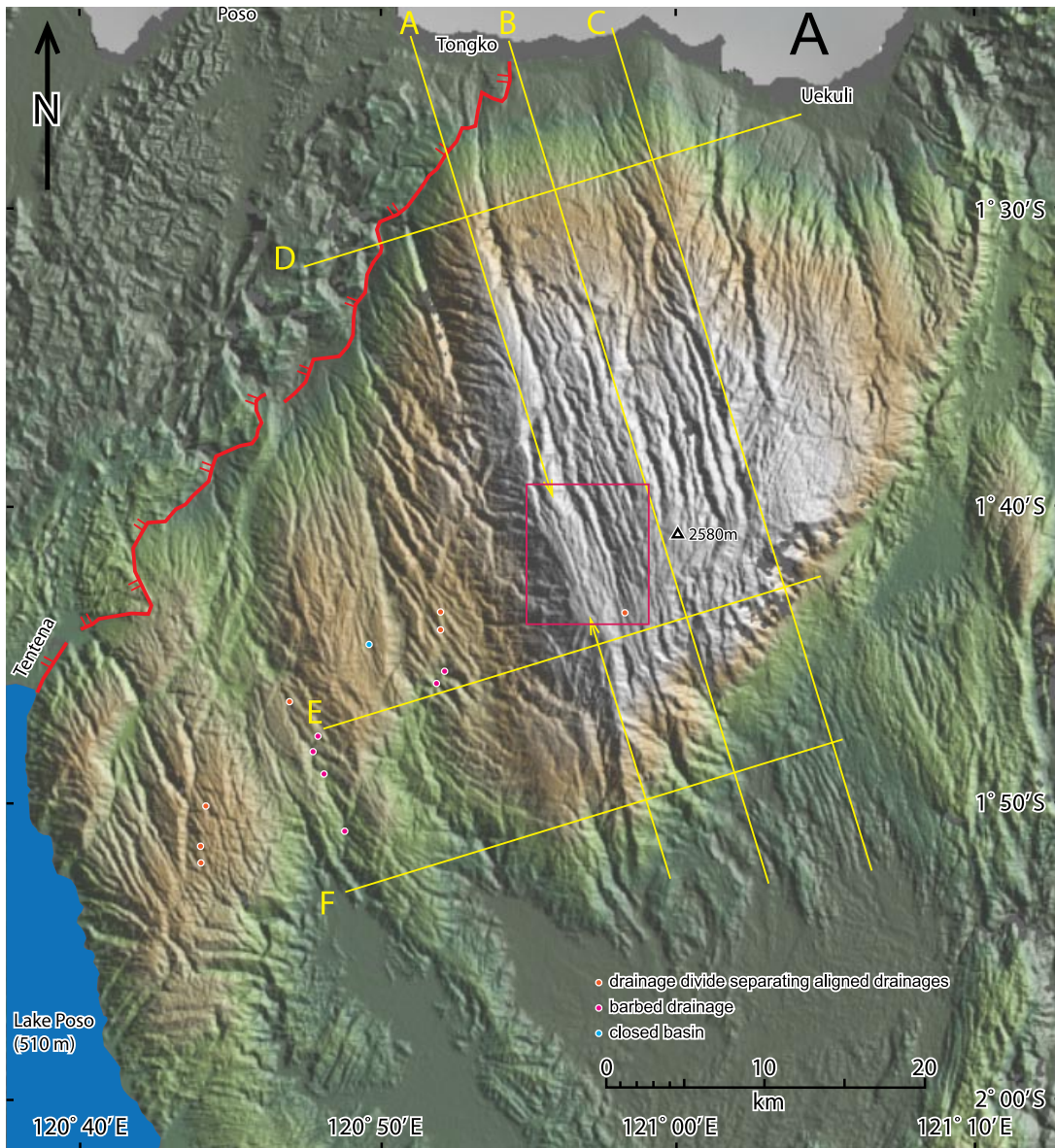
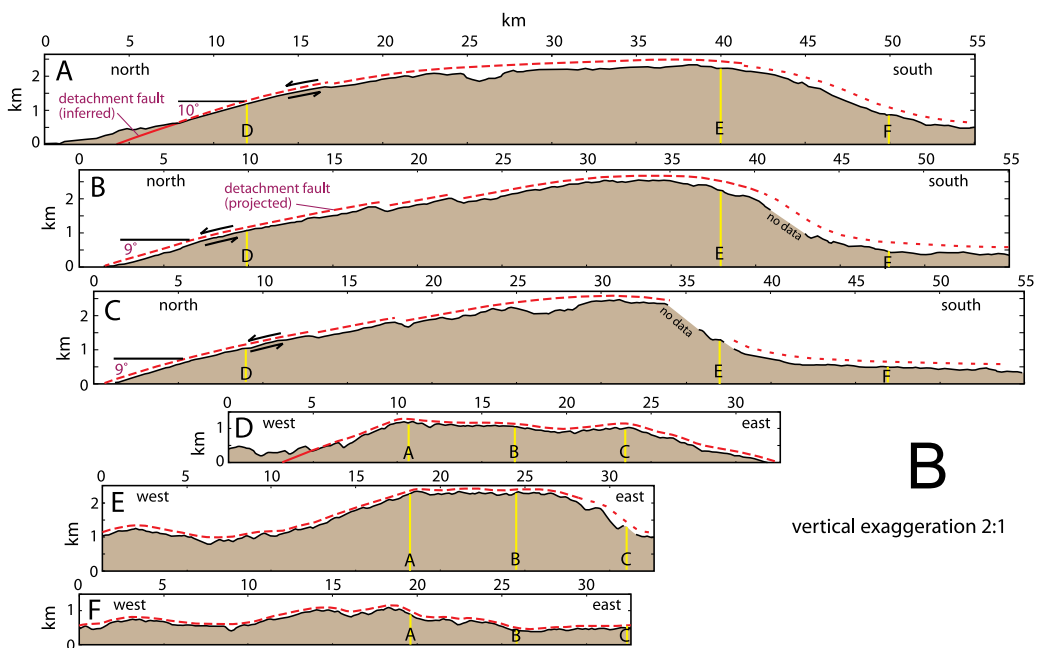


Figure 12. (A) Pompangeo Mountains and surrounding areas in central Sulawesi, Indonesia. Image derived from digital elevation model produced by Space Shuttle Radar Topography Mission (Farr et al., 2007) using GeoMapApp web-based data-visualization tool (www.geomapp.org). Gray area in northernmost areas is Gulf of Tomini. Inferred detachment fault is shown with red line with double ties on hanging-wall block. Red-outline box is area of aerial-photograph in Hamilton (1979, Fig. 86) and in Parkinson (1998, Fig. 6). (B) Cross sections created using the GeoMapApp web-based data-visualization tool (www.geomapp.org). Vertical exaggeration is 2:1. Cross-section locations are shown in Figure 12A.



originally upstream segments. We interpret this reversal as a response to isostatic uplift and arching during tectonic denudation (Spencer, 1984, 2000). The steep southeastern slope flanking the high, central part of the massif is plausibly due to monoclonal folding in response to concave-upward bending of the massif during exhumation and uplift (e.g., Spencer, 1982, 1985; Spencer and Reynolds, 1991).

The grooved Pompageo massif is exposed over at least 40 km parallel to groove axes, which is the minimum amount of detachment-fault displacement necessary to uncover the complex. The most obvious corrugation of the massif is the west flank of the central, high-elevation part of the massif just west of cross-section A. Cross-sections D and E show the westward slope on the groove flank, with ~1200 m of relief on cross-section E. This lateral ramp extends along trend for ~30 km, but south of cross-section E gradually changes form and is largely absent on cross-section F. If the Pompageo massif is interpreted correctly as a metamorphic core complex, or at least as the exhumed footwall of a detachment fault, then this 30-40 km long, west-sloping surface reflects an irregularity in the bounding detachment fault that persisted during 30-40 km of displacement and footwall exhumation. This corrugated footwall form, and other, parallel grooves, were possibly shaped by tectonic continuous casting, at least in northern exposures where the most deeply exhumed rocks would be expected.

Rincon Mountains, southeastern Arizona, USA. The southwest-dipping Catalina detachment fault separates the Rincon and Santa Catalina Mountains from Tucson basin to the southwest (Fig. 13; Drewes, 1977; Dickinson, 1991, 1999; Richard et al., 2005). Granitic and gneissic rocks that make up the fault footwall are overprinted by a mylonitic fabric that, in most areas, is parallel to the upward projection of the detachment-fault surface. The mylonitic fabric is strongly lineated and asymmetric petrofabrics generally indicate a top-southwest sense of shear (Davis, 1980; Perry, 2005; Spencer, 2006). Farther northeast, away from the foot of the ranges, the Tertiary mylonitic fabric is weak or absent. On the northeastern flank of the ranges, Proterozoic and Paleozoic metasedimentary rocks dip northeastward and represent the top of a tilted upper- to middle-crustal section (Lingrey, 1982; Bykerk-Kauffman, 2008), with the deepest exposures represented by the mylonitic gneiss and granite at the southwest foot of the ranges. Oligocene and lower Miocene hanging-wall strata, in some cases with fanning-dip sequences, were deposited in extensional basins above the active detachment fault (Dickinson, 1991). Fission-track, helium-apatite, and K-Ar (illite) dates that record cooling due to footwall exhumation are generally early to middle Miocene (Fayon et al., 2000; Damon and Shafiqullah, 2006; Andy Gleadow, written communication, 2006). The two ranges were further uplifted by displacement on two late Miocene to Pliocene high-angle normal faults (Davis et al., 2004).

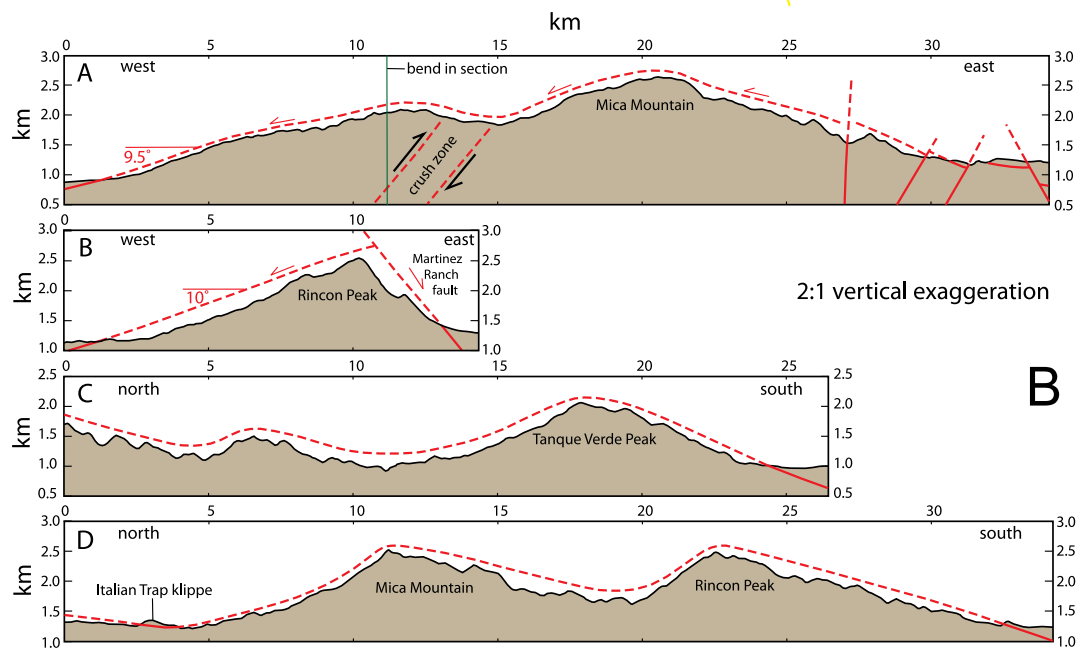
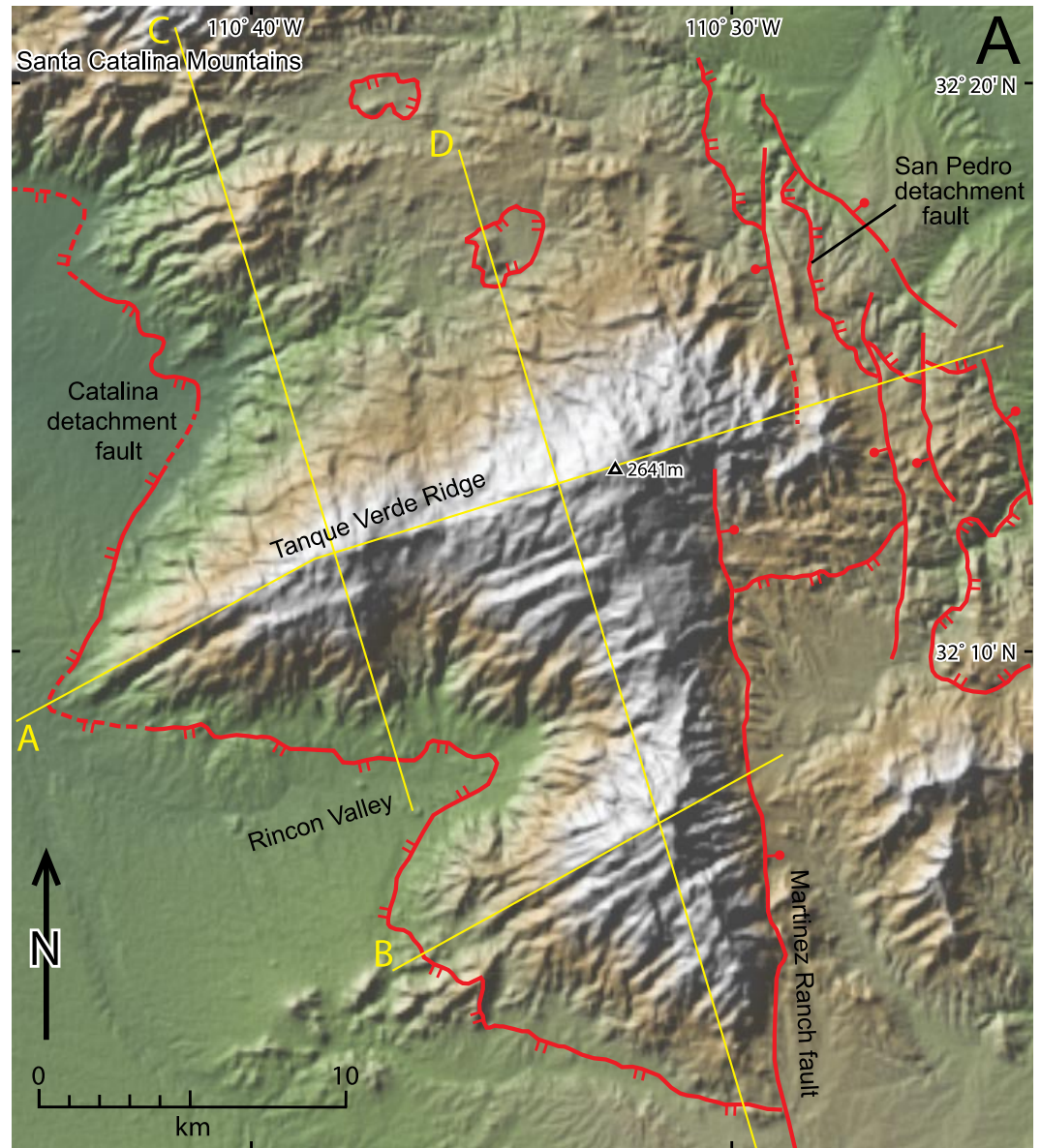
The Catalina detachment fault wraps around the south end of the Rincon Mountains where it is cut by the high-angle Martinez Ranch normal fault. Its offset continuation to the

east is known as the San Pedro detachment fault (Fig. 13). Both the Catalina and San Pedro detachment faults form the upward-bounding low-angle fault to the Rincon core complex and both place unmetamorphosed Oligo-Miocene strata (and diverse other rock types) over penetratively deformed footwall rocks (Drewes, 1977; Lingrey, 1982; Thorman and Drewes, 1981; Richard et al., 2005; Spencer et al., 2008a, b). The faults were correlative early in faulting history, but as uplift of the Rincon Mountains proceeded and the range became an impediment to further displacement of hanging-wall rocks on the northeast side of the ranges, displacement ended on the San Pedro fault, a secondary breakaway developed, and exhumation of the range continued during displacement on the Catalina detachment fault (Spencer, 1984). Mylonitic footwall rocks uncovered during this late phase of extensional exhumation provided a source of clastic debris shed into the growing Tucson basin and sub-basins during continued faulting and tilting (Dickinson, 1999; Spencer et al., 2005).

Rocks directly beneath detachment faults are commonly brecciated and chloritically altered over several to several tens of meters downward, with decreasing severity at greater distances from the fault (e.g., Davis et al., 1980; Rehrig and Reynolds, 1980). Significant fracturing commonly extends many tens of meters structurally downward. Hematite staining along fractures within the brecciated and fractured footwall rocks reveal the influx of oxidizing groundwater with meteoric oxygen-isotopic signatures following chloritic alteration and associated brecciation (e.g., Reynolds and Lister, 1987; Smith et al., 1991). Fractured rocks beneath the Catalina detachment fault are poorly resistant and have been removed by erosion from resistant crystalline footwall rocks that comprise bedrock exposures in most of the ranges (Pain, 1985). This is especially apparent in the development of a flat, low-relief surface at the foot of the western Rincon Mountains, typically hundreds of meters to a kilometer wide, that separates the detachment fault from resistant, unaltered and unbrecciated footwall rocks (Fig. 13). The resistant core of the Rincon Mountains is marked by perhaps a dozen drainages that parallel the west-southwest-trending mylonitic lineations and the broadly corrugated form of the range (Fig. 13; Pain, 1985; Spencer, 2000), including drainages perched along the crest of Tanque Verde Ridge as along antiforms at Dayman dome and the Pompageo Mountains.

Tanque Verde Ridge in the northern Rincon Mountains makes up one of the largest known core-complex corrugations. Footwall rocks exposed along its axis for ~30 km include leucogranite over the entire groove length, and metasedimentary tectonites at the eastern end. These rock types contrast with unmetamorphosed to weakly metamorphosed hanging-wall rocks at both ends of the ridge. The absence of hanging-wall equivalents of footwall rock units anywhere around the Rincon Mountains requires many tens of kilometers of detachment-fault displacement so that hangingwall equivalents of footwall leucogranite and tectonites must have been displaced southwestward to beneath Tucson basin. The 30 km distance

Figure 13. (A) Rincon Mountains in southeastern Arizona, USA. Image derived from digital elevation model produced by Space Shuttle Radar Topography Mission (Farr et al., 2007) using GeoMapApp web-based data-visualization tool (www.geomapapp.org). Faults are shown with red lines; detachment faults with double tics on hanging-wall block, moderate to high-angle normal faults with bar and ball on hanging-wall block. The Tucson metropolitan area is directly left of the imaged area. (B) Cross sections created using the GeoMapApp web-based data-visualization tool (www.geomapapp.org). Vertical exaggeration is 2:1. Cross-section locations are shown in Figure 13A. Reverse shear zone shown in cross section A is based on monoclinial folding of footwall foliation and detachment fault (Richard et al., 2005).



over which contrasting footwall and hanging-wall rocks are exposed is the minimum displacement. Forty or more kilometers of displacement are plausible.

A prediction of continuous-casting theory for the origin of core-complex corrugations is that plastically deforming middle-crustal rocks, where introduced to the stronger and colder, grooved underside of the hanging wall during extension, should flow into antiformal grooves and away from synformal grooves. Accordingly, mylonitic-lineation trend, while parallel to groove axes along antiform crests and synform troughs, might reveal deep-crustal flow converging toward antiforms. This should be most apparent about mid-way between corrugation crest and trough. Perry (2005) evaluated lineation orientations across the crest of the southwestern end of Tanque Verde Ridge and extending about one fourth of the way down the ridge flanks toward trough axes, but found no evidence of the lineation-trend variations predicted by continuous-casting theory. While a positive result from this study would be strongly supportive, the negative result can be reconciled with continuous-casting theory because flow and molding might require greater temperature and lower rock strength than that associated with mylonitic-lineation genesis. In this case, mylonitization occurred largely or entirely during the latest plastic footwall deformation just before transition to brittle conditions, and after bulk flow during molding (if it occurred at all). This is plausible because the most visible and easily measured lineations seem to be those that were subjected to the greatest grain-size reduction during mylonitization, and greater grain-size reduction would be expected when temperatures are lower.

Harcuvar core complex, western Arizona, USA. The Harcuvar metamorphic core complex of western Arizona consists of six antiformal grooves and intervening synforms, all bounded above by a detachment fault with top-east-northeast displacement (Fig. 14). In the Buckskin Mountains in the northern part of the Harcuvar core complex, 39 km of mylonitic footwall are exposed in the direction of extension, which is a minimum amount of displacement necessary to uncover the Oligo-Miocene mylonite zone and its middle crustal host gneisses and granitoids (Spencer and Reynolds, 1991). The Harcuvar Mountains make up a single, 50-km-long antiformal groove. The eastern two thirds of the range contain a well lineated mylonitic fabric that dies out gradually westward. Lineations parallel the axis of the antiform and both trend slightly more easterly at the east end of the range. Mylonitic foliation in the easternmost Harquahala Mountains similarly dies out westward, but only a small fraction of the range is mylonitic (Richard et al., 1990). The western third of the Harcuvar Mountains and the western three fourths of the Harquahala Mountains are unmylonitized and have yielded a variety of mica K-Ar dates between 43 and 72 Ma (Rehrig and Reynolds, 1980; Reynolds et al., 1986). These dates pre-date tectonic exhumation and indicate that the western parts of these ranges were above the brittle-ductile transition when lithospheric extension began at about 28 Ma.

The regular spacing and fold-like topographic form of five of the six antiformal corrugations that make up the Harcuvar core complex (the Harquahala Mountains are more geometrically complex), and the crudely corrugated form of gneissic layering and granite sills, led to early interpretation of the corrugations as folds (e.g., Cameron and Frost, 1981; Spencer, 1982). However, no other structures, such as reverse or thrust faults, have been identified that support shortening associated with folding (e.g., Spencer and Reynolds, 1989; Drewes et al., 1990; Reynolds and Spencer, 1993; Bryant, 1995; Scott, 2004). The extensive, western, non-mylonitic part of the Harcuvar Mountains in particular does not seem to be a fold, but rather is a single massif of late Cretaceous granite and older crystalline rocks. The western Harcuvar Mountains grade eastward into the eastern Harcuvar Mountains where the crystalline core of granite and gneiss is mantled by a mylonitic foliation that forms an arch-like shear zone at high structural levels. Rather than a fold, the range is a single long ridge of crystalline rock broken by a several minor Tertiary high-angle faults that cut across the range, and is bounded at the foot of the range in eastern exposures by a detachment fault.

The obvious interpretation of the structure of the Harcuvar Mountains is that the range is an antiformal groove of the detachment fault, and that the western part of the range is a groove that developed in the brittle upper crust as a promontory in a range-front normal fault, as is typical of normal faults (Jackson and White, 1989). The now tilted and flattened normal-fault footwall exposes the brittle-ductile transition in the central part of the range that was originally down-dip from the range-front normal fault. The eastern part of the range either developed as the footwall of a corrugated mylonitic shear zone simultaneously over its entire length, or it flowed into a position below a corrugated mylonitic shear zone directly down dip from a nearby corrugated normal fault, and received its corrugated form by molding to the stronger and colder, grooved underside of the hanging-wall. The great length of the corrugated mylonitic shear zones (30-40 km) in the Harcuvar core complex suggest flow rather than simultaneous development of a corrugated mylonitic shear zone extending at least this distance laterally in the middle crust.

DISCUSSION AND CONCLUSION

Subaerial extrusion of viscous magma from volcanoes and in “squeeze-ups” has produced striated surfaces, as has submarine flow of basaltic magma from beneath seafloor lava-lake crusts. Striations range from millimeters to meters in wavelength, and decimeters to tens to perhaps hundreds of meters in length. While fissure-related squeeze-ups and extrusions from volcanoes are surrounded by striations, striations produced by flow of submarine lava from beneath lava-lake crusts, or during slip between partially molten lava-crust fragments, are only striated on one side. The molding rocks that presumably produced the striations at Sacsayhuamán are not exposed in contact with the extrusion but plausibly consist

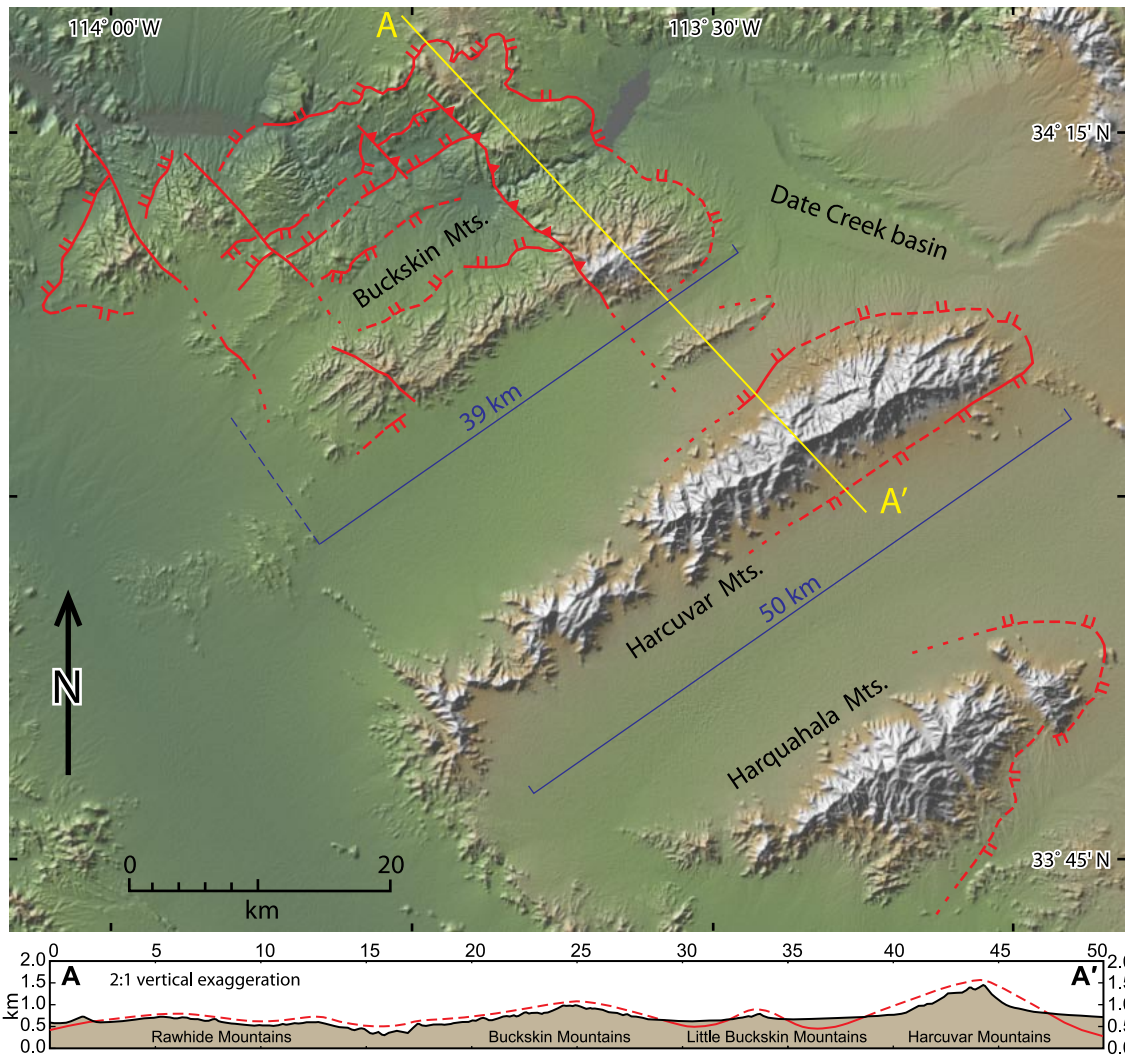


Figure 14. (A) Harcuvar core complex in western Arizona, USA. Image derived from digital elevation model produced by Space Shuttle Radar Topography Mission (Farr et al., 2007) using GeoMapApp web-based data-visualization tool (www.geomapapp.org). Faults are shown with red lines; detachment faults with double tics on hanging-wall block, reverse faults with teeth on hanging-wall block. Cross section created using GeoMapApp web-based data-visualization tool (www.geomapapp.org). Vertical exaggeration is 2:1.

of nearby carbonates. The form of the extrusion suggests that it was uncovered by lateral displacement of overlying rocks. In this case the striated extrusion is grooved on only one side, as with submarine lava striated during flow from beneath lava crusts. Regardless of whether lava is striated on one side or forms extrusions surrounded by striations, the geologic process of producing linear forms in cooling and solidifying magmas adjacent to a slip surface is analogous to the widely used industrial process of continuous casting.

Grooved deep-sea metamorphic core complexes resemble grooved lavas but are much larger (Table 1). Three deep-sea core complexes penetrated by drill holes consist largely or dominantly of gabbro, indicating that magmatism was important in constructing the exhumed footwall blocks (Dick et al., 2000; Keleman et al., 2004; Blackman et al., 2006). Tucholke et al. (2008) concluded that (1) the brittle-ductile transition

above magma chambers localizes fault formation, (2) irregularities in this transition related to intrusion geometry determine the cross-sectional shape of footwall grooves, (3) once established, “the cool hanging-wall mold could continue

Table 1. Geometric characteristics of core complexes

core complex	max groove length (km)	groove half-wavelength* (km)	groove amplitude (km)	normal-fault dip
Godzilla	60	0.7 - 13	0.1 - 1.5	
Wasatch	7	~10	~1 - 2	21-28°
Dayman	20	~10 - 20	0.5 - 1.5	18-23°
Pompageo	30	8 - 15	0.2 - 1.0	9°
Rincon	30	7 - 15	0.5 - 1.5	10°
Harcuvar	50	6 - 12	0.2 - 1.0	10°

*measured trough-to-trough or crest-to-crest

to shape the exhuming footwall (with or without magmatic injection)", and (4) too much or too little magmatism prevents development of long-lived detachments. The remarkably long grooves of some deep-sea core complexes, best represented by the 60-km-long groove at the Godzilla Mullion, reveal the great stability of fault geometry and associated consistency of thermal conditions and mechanical properties during substantial lithospheric extension. This stability appears to involve coupling of magmatic and tectonic processes, perhaps with a consistent but not overwhelming magma supply providing, along with hot wall rocks, a pliable medium for continuous casting. Understanding the details of this process is a first-order challenge in understanding oceanic-lithosphere divergence.

Range-front normal faults such as the Wasatch front in western USA typically include promontories and embayments that represent fault-surface irregularities. With sufficient displacement, normal faults exhume footwall mylonites that were produced down-dip from the fault (e.g., Davis et al., 1986). Normal-fault exhumation of middle crustal rocks does not occur unless faults are gently dipping or become so due to footwall tilting and flattening. Mylonitic footwalls uplifted and tilted to gently dips during tectonic exhumation are commonly grooved. These grooves are most simply interpreted as normal-fault irregularities projected into the middle crust (Jackson and White, 1989). Interpretation of grooves simply as down-dip continuations of fault corrugations is problematic if grooves are tens of kilometers long (Table 1), as this would require simultaneous development of a grooved mylonitic shear zone over tens of kilometers laterally in the middle crust. Alternatively, the middle crust flows into the extending zone and is tectonically cast into grooves before entering the brittle regime during exhumation-related cooling (Spencer and Reynolds, 1991; Spencer, 1999).

The four continental core complexes discussed in this paper all have long and/or well-developed grooves (Table 1) and are intended to serve as some of Earth's best examples of grooved footwalls. These are also potential targets of future studies to determine if mid-crustal flow paths conform to expectations for continuous casting, although for Dayman dome and, especially, for the Pompageo Schist Complex, studies are needed just to demonstrate that the areas are mylonitized in a manner expected for a core complex. Perry's (2005) study, intended to determine if flow paths conform to expectations for continuous casting, produced negative but not definitive results. Bulk strains required for continuous casting are not large, resulting, for example, in a few percent increase in shear-zone surface area associated with molding. It thus might be difficult to identify strains associated with tectonic continuous casting. Another confounding factor might be that molding occurs largely or entirely before mylonitization. It is not uncommon in Arizona, for example, to find isoclinal folds in gneissic rocks with axes oriented approximately parallel to mylonitic lineation. These folds developed at temperatures higher than those associated with mylonitization and are plau-

sibly associated with bulk strain that occurred during molding to an overlying, corrugated shear zone. As with deep-sea core complex corrugations, understanding the process of long-groove genesis will require much further research.

ACKNOWLEDGMENTS

We thank Bill Chadwick for photographs of submarine lineated sheet flows, Roland Brady for photographs of lineated outcrops at Sacsayhuamán, and John Bartley for review comments about the Wasatch Front. This paper represents a talk given at the AGS Ores and Orogenesis Symposium in place of a no-show.

REFERENCES CITED

- Armstrong, P.A., Taylor, R.A., and Ehlers, T.A., 2004, Is the Wasatch fault footwall (Utah, United States) segmented over million-year time scales?: *Geology*, v. 32, n. 5, p. 385–388; doi: 10.1130/G20421.1
- Baldwin, S.L., Monteleone, B., Webb, L.E., Fitzgerald, P.G., Grove, M. and Hill, E.J., 2004, Pliocene eclogite exhumation at plate tectonic rates in eastern Papua New Guinea: *Nature*, v. 431, p. 263–267.
- Bates, R.L., and Jackson, J.A., eds., 1980, *Glossary of geology*, 2nd ed., Falls Church, Virginia, American Geological Institute, 751 p.
- Bellier, O., Sebrier, M., Seward, D., Beaudouin, T., Villeneuve, M., 2006, Fission track and fault kinematics analyses for new insight into the late Cenozoic tectonic regime changes in west-central Sulawesi (Indonesia): *Tectonophysics*, v. 413, n. 3-4, p. 201-220.
- Blackman, D.K., Cann, J.R., Janssen, Bob, and Smith, D.K., 1998, Origin of extensional core complexes: Evidence from the Mid-Atlantic Ridge at Atlantis Fracture Zone: *Journal of Geophysical Research*, v. 103, p. 21,315-21,333.
- Blackman, D.K., Ildefonse, B., John, B.E., Ohara, Y., Miller, D.J., MacLeod, C.J., and Expedition 304/305 Scientists, 2006, *Proceedings of the Integrated Ocean Drilling Program, Volume 304/305*: College Station, Texas, Integrated Ocean Drilling Program, doi: 10.2204/iodp.proc.304305.2006.
- Block, L., and Royden, L.H., 1990, Core-complex geometries and regional scale flow in the lower lithosphere: *Tectonics*, v. 9, p. 557-567.
- Bruhn, R.L., Gibling, P.R., and Parry, W.T., 1987, Rupture characteristics of normal faults – an example from the Wasatch fault zone, Utah, *in* Coward, M.P., Dewey, J.F., and Hancock, P.L., eds., *Continental extensional tectonics*: Geological Society Special Publication 28, p. 333-353.
- Bryant, B., 1995, *Geologic map, cross-sections, isotopic dates, and mineral deposits of the Alamo Lake 30' x 60' quadrangle, west-central Arizona*: U.S. Geological Survey Miscellaneous Investigations Series Map I-2489, 3 sheets, scale 1:100,000.
- Buck, W.R., 1988, Flexural rotation of normal faults: *Tectonics*, v. 7, p. 959-973.
- Bykerk-Kauffman, A., 2008, *Geologic map of the northeastern Santa Catalina Mountains, Pima County, Arizona*: Arizona Geological Survey Contributed Map CM-08-A, scale 1:24,000.
- Cameron, T. E., and Frost, E. G., 1981, Regional development of major antiforms and synforms coincident with detachment faulting in California, Arizona, Nevada, and Sonora [abs.]: *Geological Society of America Abstracts with Programs*, v. 13, p. 421-422.

- Cann, J.R., Blackman, D.K., Smith, D.K., McAllister, E., Janssen, B., Mello, S., Aygerinos, E., Pascoe, A.R., and Escartin, J., 1997, Corrugated slip surfaces formed at ridge-transform intersections on the Mid-Atlantic Ridge: *Nature*, v. 385, p. 329-332.
- Cannat, M., 1993, Emplacement of mantle rocks in the seafloor at mid-ocean ridges: *Journal of Geophysical Research*, v. 98, p. 4,163-4,172.
- Cannat, M., Mével, C., and Stakes, D., 1991, Stretching of the deep crust at the slow-spreading southwest Indian ridge: *Tectonophysics*, v. 190, p. 73-94.
- Chadwick, W.W., Jr., Gregg, T.K.P., and Embley, R.W., 1999, Submarine lineated sheet flows: A unique lava morphology formed on subsiding lava ponds: *Bulletin of Volcanology*, v. 61, p. 194-206.
- Christie, D.M., West, B.P., Pyle, D.G., and Hanan, B.B., 1998, Chaotic topography, mantle flow and mantle migration in the Australian-Antarctic discordance: *Nature*, v. 394, p. 637-644; doi: 10.1038/29226.
- Colton, H.S., and Park, C.F., Jr., 1930, Anosma or "squeeze-ups": *Science*, v. 72, n. 1875, p. 579.
- Crittenden, M.D., Jr., Coney, P.J., and Davis, G.H., eds., 1980, Cordilleran metamorphic core complexes: *Geological Society of America Memoir 153*, 490 p.
- Daczko, N.R., Caffi, P., Carroll, S.A., 2007, Exhumation of the Suckling-Dayman Massif, Papua New Guinea: *Eos, Transactions of the American Geophysical Union, Supplement*, Abstract T41C-05.
- Damon, P.E., and Shafiqullah, M., 2006, K-Ar dates of fault rocks along the Catalina detachment fault, Tanque Verde Ridge, Rincon Mountains, Arizona: *Arizona Geological Survey Contributed Report CR-06-A*, 18 p.
- Davies, H.L., 1980, Folded thrust fault and associated metamorphics in the Suckling-Dayman Massif, Papua New Guinea, *in* Irving, A.J., and Dungan, M.A., eds., *The Jackson volume: American Journal of Science*, v. 280-A, p. 171-191.
- Davis, F.D., compiler, 1983a, Geologic map of the central Wasatch Front, Utah: *Utah Geological and Mineral Survey Map 54-A*, scale 1:100,000.
- Davis, F.D., compiler, 1983b, Geologic map of the southern Wasatch Front, Utah: *Utah Geological and Mineral Survey Map 55-A*, scale 1:100,000.
- Davis, G.A., and Lister, G.S., 1988, Detachment faulting in continental extension; Perspectives from the southwestern U.S. Cordillera, *in* Clark, S.P., Jr., Burchfiel, B.C., and Suppe, J., eds., *Processes in continental lithosphere deformation: Geological Society of America Special Paper 218*, p. 133-160.
- Davis, G.A., Anderson, J.L., Frost, E.G., and Shackelford, T.J., 1980, Mylonitization and detachment faulting in the Whipple-Buckskin-Rawhide Mountains terrane, southeastern California and western Arizona, *in* Crittenden, M.D., Jr., Coney, P.J., and Davis, G.H., eds., *Cordilleran metamorphic core complexes: Geological Society of America Memoir 153*, p. 79-129.
- Davis, G.A., Lister, G. S., and Reynolds, S. J., 1986, Structural evolution of the Whipple and South Mountains shear zones, southwestern United States: *Geology*, v. 14, p. 7-10.
- Davis, G.H., 1980, Structural characteristics of metamorphic core complexes, southern Arizona, *in* Crittenden, M.D., Jr., Coney, P.J., and Davis, G.H., eds., *Cordilleran metamorphic core complexes: Geological Society of America Memoir 153*, p. 35-77.
- Davis, G.H., Constenius, K.N., Dickinson, W.R., Rodríguez, E.P., and Cox, L.J., 2004, Fault and fault-rock characteristics associated with Cenozoic extension and core-complex evolution in the Catalina-Rincon region, southeastern Arizona: *Geological Society of America Bulletin*, v. 116, n. 1/2, p. 128-141.
- Dick, H.J.B., Natland, J.H., Alt, J.C., Bach, W., Bideau, D., Gee, J.S., Haggas, S., Hertogen, J.G.H., Hirth, G., Holm, P.M., Ildefonse, B., Iturrino, G.J., John, B.E., Kelley, D.S., Kikawa, E., Kingdon, A., LeRoux, P.J., Maeda, J., Meyer, P.S., Miller, D.J., Naslund, H.R., Niu, Y., Robinson, P.T., Snow, J., Stephan, R.A., Trimby, P.W., Worm, H., Yoshinobu, A., 2000, A long in situ section of the lower ocean crust: Results of ODP Leg 176 drilling at the Southwest Indian Ridge: *Earth and Planetary Science Letters*, v. 179, p. 31-51.
- Dickinson, W.R., 1991, Tectonic setting of faulted Tertiary strata associated with the Catalina core complex in southern Arizona: *Geological Society of America, Special Paper 264*, 106 p.
- Dickinson, W.R., 1999, Geologic framework of the Catalina foothills, outskirts of Tucson (Pima County, Arizona): *Arizona Geological Survey Contributed Map CM-99-B*, scale 1:24,000, 31 p.
- Drewes, H., 1977, Geologic map and sections of the Rincon Valley Quadrangle, Pima County, Arizona: *U.S. Geological Survey Miscellaneous Investigations Series Map I-997*, scale 1:48,000.
- Drewes, H.D., DeWitt, E., Hill, R.H., Hanna, W.F., Knepper, D.H., Jr., Tuftin, S.E., Reynolds, S.J., Spencer, J.E., and Azam, S., 1990, Mineral resources of the Harcuvar Mountains Wilderness Study Area, La Paz County, Arizona, Chapter F, *in* *Mineral Resources of Wilderness Study Areas – Western Arizona and part of San Bernardino County, California: U.S. Geological Survey Bulletin 1701-F*, p. F1-F29, 1 sheet, scale 1:50,000.
- Drobia R.K., and DeMets, C., 2005, Deformation in the diffuse India-Capricorn-Somalia triple junction from a multibeam and magnetic survey of the northern Central Indian Ridge, 3°S-10°S: *Geochemistry, Geophysics, Geosystems*, v. 6, p. 9, doi: 10.1029/2005GC000950.
- Eriksen, G.E., 1986, Comment *on* June 1985 *Geology* cover: *Geology*, v. 14, p. 91-92.
- Farr, T.G., Rosen, P.A., Caro, E., Crippen, R., Duren, R., Hensley, S., Kobrick, M., Paller, M., Rodriguez, E., Roth, L., Seal, D., Shaffer, S., Shimada, J., Umland, J., Werner, M., Oskin, M., Burbank, D., and Alsdorf, D., 2007, The shuttle radar topography mission: *Reviews in Geophysics*, v. 45, doi:10.1029/2005RG000183.
- Fayon, A.K., Peacock, S.M., Stump, E., and Reynolds, S.J., 2000, Fission track analysis of the footwall of the Catalina detachment fault, Arizona: Tectonic denudation, magmatism, and erosion: *Journal of Geophysical Research*, v. 105, n. B5, p. 11,047-11,062.
- Feininger, T., 1978, The extraordinary striated outcrop at Saqsaywaman, Peru: *Geological Society of America Bulletin*, v. 89, p. 494-503.
- Feininger, T., 1980, Reply to Discussion of "The extraordinary striated outcrop at Saqsaywaman, Peru": *Geological Society of America Bulletin*, Part 1, v. 91, p. 251-252.
- Ferrill, D.A., Stamatakos, J.A., and Sims, D., 1999, Normal fault corrugation: Implications for growth and seismicity of active normal faults: *Journal of Structural Geology*, v. 21, p. 1027-1038.
- Gabelman, J.W., 1967, Structure and origin of El Rodadero, Cuzco, Perú: *Boletín de la Sociedad Geológica del Perú*: v. 40, p. 25-54.
- Gilbert, G.K., 1904, The mechanism of the Mont Pele spine: *Science*, v. 19, n. 494, p. 927-928.
- Gilbert, G.K., 1928, Studies of basin and range structure: *U.S. Geological Survey Professional Paper 153*, 92 p.
- Hall, R., 2002, Cenozoic geological and plate tectonic evolution of SE Asia and the SW Pacific: computer-based reconstructions, model and animations: *Journal of Asian Earth Sciences*, v. 20, p. 353-434.
- Hall, R., 2008, Continental growth at the Indonesian margins of SE Asia, *in* Spencer, J.E., and Tittley, S.R., eds., *Ores and orogenesis: Circum-Pacific tectonics, geologic evolution, and ore deposits: Arizona Geological Society Digest 22*, p. 245-258.

- Hamilton, W., 1979, Tectonics of the Indonesia region: U.S. Geological Survey Professional Paper 1078, 345 p., *with* Tectonic map of Indonesia, scale 1:5,000,000.
- Harigane, Y., Michibayashi, K., and Ohara, Y., 2008, Shearing within lower crust during progressive retrogression: Structural analysis of gabbroic rocks from the Godzilla Mullion, an oceanic core complex in the Parece Vela backarc basin: *Tectonophysics*, v. 457, p. 183-196.
- Herrmann, E., 1980, *Handbook on continuous casting*: Düsseldorf, Aluminium-Verlag, 742 p.
- Hill, E.J., Baldwin, S.L., and Lister, G.S., 1992, Unroofing of active metamorphic core complexes in the D'Entrecasteaux Islands, Papua New Guinea: *Geology*, v. 20, p. 907-910.
- Hovey, 1903, The new cone of Mont Pelé and the Gorge of the Rivière Blanche, Martinique: *American Journal of Science*, v. 16, n. 94, p. 268-281.
- Iverson, R.M., Dzurisin, D., Gardner, C.A., Gerlach, T.M., LaHusen, R.G., Lisowski, M., Major, J.J., Malone, S.D., Messerich, J.A., Moran, S.C., Pallister, J.S., Qamar, A.I., Schilling, S.P., Vallance, J.W., 2006, Dynamics of seismogenic volcanic extrusion at Mount St Helens in 2004–05: *Nature*, v. 444, p. 439-443; doi:10.1038/nature05322.
- Jackson, J.A., and White, N.J., 1989, Normal faulting in the upper continental crust: observations from regions of active extension: *Journal of Structural Geology*, v. 11, p. 15-36.
- Jaroslow, G.E., Hirth, G., and Dick, H.J.B., 1996, Abyssal peridotite mylonites: implications for grain-size sensitive flow and strain localization in the oceanic lithosphere: *Tectonophysics*, v. 256, p. 17-37.
- Karson, J.A., and Dick, H.J.B., 1983, Tectonics of ridge-transform intersections at the Kane fracture zone: *Marine Geophysical Researches*, v. 6, p. 51-98.
- Kasuga, S. and Ohara, Y., 1997, A new model of back-arc spreading in the Parece Vela Basin, northwest Pacific margin: *The Island Arc*, v. 6, p. 316–326.
- Kelemen, P.B., Kikawa, E., Miller, D.J., and Shipboard Scientific Party, 2004, Proceedings of the Ocean Drilling Program, Initial Reports, v. 209: College Station, Texas, Ocean Drilling Program, doi: 10.2973/odp.proc.ir.209.2004.
- Lingrey, S.H., 1982, Structural geology and tectonic evolution of the northeastern Rincon Mountains, Cochise and Pima Counties, Arizona: Tucson, University of Arizona, unpublished Ph.D. thesis, 202 p.
- Little, T.A., Baldwin, S.L., Fitzgerald, P.G., and Monteleone, B., 2007, Continental rifting and metamorphic core complex formation ahead of the Woodlark spreading ridge, D'Entrecasteaux Islands, Papua New Guinea: *Tectonics*, v. 26, doi:10.1029/2005TC001911.
- Machette, M.N., Personius, S.F., Nelson, A.R., Schwartz, D.P., and Lund, W.R., 1991, The Wasatch fault zone, Utah – segmentation and history of Holocene earthquakes: *Journal of Structural Geology*, v. 13, n. 2, p. 137-149.
- Marocco, R., 1980, The extraordinary striated outcrop at Saqsaywaman, Peru: Discussion: *Geological Society of America Bulletin*, v. 91, p. 251.
- Martínez, F., Taylor, B., and Goodliffe, A.M., 1999, Contrasting styles of seafloor spreading in the Woodlark Basin: Indications of rift-induced secondary mantle convection: *Journal of Geophysical Research*, v. 104, n. B6, p. 12,909–12,926.
- Neuendorf, K.K.E., Mehl, J.P., Jr., and Jackson, J.A., eds., 2005, *Glossary of geology*: American Geological Institute, 5th ed., 779 p.
- Nichols, R.L., 1938, Grooved lava: *Journal of Geology*, v. 46, p. 601-614.
- Ohara, Y., Yoshida, T., Kato, Y., and Kasuga, S., 2001, Giant megamullion in the Parece Vela backarc basin: *Marine Geophysical Researches*, v. 22, p. 47-61.
- Ohara, Y., Fujioka, K., Ishii, T., and Yurimoto, H., 2003a, Peridotites and gabbros from the Parece Vela backarc basin: Unique tectonic window in an extinct backarc spreading ridge: *Geochemistry, Geophysics, Geosystems*, v. 4, n. 7, p. 8611, doi:10.1029/2002GC000469.
- Ohara, Y., Okino, K., Snow, J.E., and KR03-01 Shipboard Scientific Party, 2003b, Preliminary report of Kairei KR03-01 cruise: Amagmatic tectonics and lithospheric composition of the Parece Vela Basin: *InterRidge News*, v. 12, n. 1, p. 27-29.
- Ohara, Y., Okino, K., Snow, J.E., and KH07-2 Science Party, 2007, IODP Site Survey for drilling Godzilla Mullion: preliminary report of R/V Hakuho KH07-2 Leg 2 & 4 cruise: EOS, Transactions of the American Geophysical Union, 88(52) Fall Meeting supplement, abstract T53B-1314.
- Okino, K., Kasuga, S., and Ohara, Y., 1998, A new scenario of the Parece Vela Basin genesis: *Marine Geophysical Researches*, v. 20, n. 1, p. 21-40.
- Okino, K., Matsuda, K., Christie, D.M., Nogi, Y., and Koizumi, K., 2004, Development of oceanic detachment and asymmetric spreading at the Australian-Antarctic discordance: *Geochemistry, Geophysics, Geosystems*, v. 5, n. 12, doi:10.1029/2004GC000793.
- Ollier, C.D., and Pain, C.F., 1980, Actively rising surficial gneiss domes in Papua New Guinea: *Journal of the Geological Society of Australia*, n. 27, p. 33-44.
- Ollier, C.D., and Pain, C.F., 1981, Active gneiss domes in Papua New Guinea - new tectonic landforms: *Zeitschrift fuer Geomorphologie*, v. 25, n. 2, p. 133-145.
- Pain, C.F., 1985, Cordilleran metamorphic core complexes in Arizona: A contribution from geomorphology: *Geology*, v. 13, p. 871-874.
- Parkinson, C., 1998, An outline of the petrology, structure and age of the Pompangeo Schist Complex of central Sulawesi, Indonesia: *The Island Arc*, v. 7, n. 1-2, p. 231-245.
- Parry, W.T., and Bruhn, R.L., 1987, Fluid inclusion evidence for minimum 11 km vertical offset on the Wasatch fault, Utah: *Geology*, v. 15, p. 67-70.
- Perry, E.R., 2005, Field and petrographic analysis of mylonitic fabrics: Implications for tectonic corrugation development, Tanque Verde Ridge, Arizona, USA: M.S. thesis, The University of Texas at Austin, 207 p.
- Rehrig, W.A., and Reynolds, S.J., 1980, Geologic and geochronologic reconnaissance of a northwest-trending zone of metamorphic core complexes in southern and western Arizona, *in* Crittenden, M.D., Jr., Coney, P.J., and Davis, G.H., eds., *Cordilleran metamorphic core complexes*: Geological Society of America Memoir 153, p. 131-157.
- Reynolds, S.J., 1985, Geology of the South Mountains, central Arizona: Arizona Bureau of Geology and Mineral Technology Bulletin 195, 61 p., 1 sheet, scale 1:24,000.
- Reynolds, S.J., and Lister, G. S., 1987, Structural aspects of fluid-rock interactions in detachment zones: *Geology*, v. 15, p. 362-366.
- Reynolds, S.J., and Spencer, J.E., 1993, Geologic map of the western Harcuvar Mountains, La Paz County, west-central Arizona: Arizona Geological Survey Open-File Report 93-8, 9 p., scale 1:24,000.
- Reynolds, S.J., Florence, F. P., Welty, J. W., Roddy, M. S., Currier, D. A., Anderson, A. V., and Keith, S. B., 1986, Compilation of radiometric age determinations in Arizona: Tucson, Arizona Bureau of Geology and Mineral Technology Bulletin 197, 258 p.

- Richard, S.M., Fryxell, J.E., and Sutter, J.F., 1990, Tertiary structure and thermal history of the Harquahala and Buckskin Mountains, west-central Arizona: Implications for denudation by a major detachment fault system: *Journal of Geophysical Research*, v. 95, p. 19,973-19,987.
- Richard, S.M., Spencer, J.E., Youberg, A., and Ferguson, C.A., 2005, Geologic map of the Rincon Valley area, Pima County, Arizona: Arizona Geological Survey Digital Geologic Map 44 (DGM-44), v. 1.0, 11 p., scale 1:24,000.
- Scott, R.J., 2004, Geologic maps and cross sections of selected areas in the Rawhide and Buckskin Mountains, La Paz and Mohave Counties, Arizona: Arizona Geological Survey Contributed Map CM-04-D, 7 sheets, various scales (1 CD-ROM).
- Silver, E.A., McCaffrey, R., Smith, R.B., 1983, Collision, rotation, and the initiation of subduction in the evolution of Sulawesi, Indonesia: *Journal of Geophysical Research*, v. 88, n. 11, p. 9407-9418.
- Smith, B.M., Reynolds, S.J., Day, H.W., and Bodnar, R., 1991, Deep-seated fluid involvement in ductile-brittle deformation and mineralization, South Mountains metamorphic core complex, Arizona: *Geological Society of America Bulletin*, v. 103, p. 559-569.
- Smith, W.H.F., and Sandwell, D.T., 1997, Global seafloor topography from satellite altimetry and ship depth soundings: *Science*, v. 277, p. 1957-1962.
- Snow, J., Ohara, Y., Hellebrand, E., Okino, K., and Ishii, T., 2004, Evolution of partial melting in intermediate/fast spreading backarc peridotites, Parece Vela Rift, Marianas backarc: *Geophysical Research Abstracts*, 6, 1607-7962/gra/EGU04-A-03894.
- Socquet, A., Simons, W., Vigny, C., McCaffrey, R., Subarya, C., Sarsito, D., Ambrosius, B., Spakman, W., 2006, Microblock rotations and fault coupling in SE Asia triple junction (Sulawesi, Indonesia) from GPS and earthquake slip vector data: *Journal of Geophysical Research*, v. 111, 15 p., B08409, doi:10.1029/2005JB003963.
- Spencer, J.E., 1982, Origin of folds of Tertiary low-angle fault surfaces, southeastern California and western Arizona, *in* Frost, E. G., and Martin, D. L., eds., *Mesozoic-Cenozoic tectonic evolution of the Colorado River region, California, Arizona, and Nevada*: San Diego, California, Cordilleran Publishers, p. 123-134.
- Spencer, J.E., 1984, Role of tectonic denudation in warping and uplift of low-angle normal faults: *Geology*, v. 12, p. 95-98.
- Spencer, J.E., 1985, Miocene low-angle normal faulting and dike emplacement at Homer Mountain and surrounding areas, southeastern California and southernmost Nevada: *Geological Society of America Bulletin*, v. 96, p. 1140-1155.
- Spencer, J.E., 1999, Geologic continuous casting below continental and deep-sea detachment faults and at the striated extrusion of Sacsayhuamán, Peru: *Geology*, v. 27, p. 327-330.
- Spencer, J.E., 2000, Possible origin and significance of extension-parallel drainages in Arizona's metamorphic core complexes: *Geological Society of America Bulletin*, v. 112, p. 727-735.
- Spencer, J.E., 2001, Possible giant metamorphic core complex at the center of Artemis Corona, Venus: *Geological Society of America Bulletin*, v. 113, p. 333-345.
- Spencer, J.E., 2003, Comment *on* Direct geologic evidence for oceanic detachment faulting: The mid-Atlantic Ridge, 15°45'N: *Geology*, online forum, p. e14.
- Spencer, J.E., 2006, A geologist's guide to the core complex geology along the Catalina Highway, Tucson area, Arizona: Arizona Geological Survey Open File Report 06-01, ver. 1.1, 38 p.
- Spencer, J.E., and Reynolds, S.J., 1989, Tertiary structure, stratigraphy, and tectonics of the Buckskin Mountains, *in* Spencer, J.E., and Reynolds, S.J., *Geology and mineral resources of the Buckskin and Rawhide Mountains, west-central Arizona*: Arizona Geological Survey Bulletin 198, p. 103-167.
- Spencer, J.E., and Reynolds, S.J., 1991, Tectonics of mid-Tertiary extension along a transect through west-central Arizona: *Tectonics*, v. 10, p. 1204-1221.
- Spencer, J.E., Ferguson, C.A., Richard, S.M., Orr, T.R., Pearthree, P.A., Gilbert, W.G., and Krantz, R.W., 2001, Geologic map of The Narrows 7 1/2' Quadrangle and the southern part of the Rincon Peak 7 1/2' Quadrangle, eastern Pima County, Arizona: Arizona Geological Survey Digital Geologic Map 10, layout scale 1:24,000, with 32 p. text (revised May, 2002).
- Spencer, J.E., Cook, J.P., Lingrey, S.H., Richard, S.M., Ferguson, C.A., and Guynn, J.H., 2008a, Geologic map of the Wildhorse Mountain 7 1/2' Quadrangle, Cochise County, Arizona: Arizona Geological Survey Digital Geologic Map DGM-62, scale 1:24,000.
- Spencer, J.E., Richard, S.M., Cook, J.P., Dickinson, W.R., Lingrey, S.H., and Guynn, J.H., 2008b, Geologic map of the Soza Canyon 7 1/2' Quadrangle, Cochise and Pima Counties, Arizona: Arizona Geological Survey Digital Geologic Map DGM-61, scale 1:24,000.
- Thorman, C.H., and Drewes, H., 1981, Geology of the Rincon wilderness study area, Pima County, Arizona, *in* Mineral Resources of the Rincon Wilderness Study Area, Pima County, Arizona: U.S. Geological Survey Bulletin 1500, p. 5-37.
- Tselikov, A.I., 1984, The continuous processing of metals in the U.S.S.R.: *Scientific American*, v. 251, n. 4, p. 120-129.
- Tucholke, B.E., Behn, M.D., Buck, W.R., and Lin, J., 2008, Role of melt supply in oceanic detachment faulting and formation of megamullions: *Geology*, v. 36, n. 6, p. 455-458.
- Tucholke, B.E., Lin, J., and Kleinrock, M.C., 1998, Megamullions and mullion structure defining oceanic metamorphic core complexes on the Mid-Atlantic Ridge: *Journal of Geophysical Research*, v. 103, p. 9857-9866.
- Villeneuve, M., Gunawan, W., Cornee, J.-J., and Vidal, O., 2002, Geology of the central Sulawesi belt (eastern Indonesia): constraints for geodynamic models: *International Journal of Earth Science*, v. 91, p. 524-537; doi: 10.1007/s005310100228
- Webb, L.E., Baldwin, S.L., Little, T.A., and Fitzgerald, P.G., 2008, Can microplate rotation drive subduction inversion?: *Geology*, v. 36, n. 10, p. 823-826; doi: 10.1130/G25134A.1
- Wernicke, B., 1992, Cenozoic extensional tectonics of the U.S. Cordillera, *in* Burchfiel, B.C., Lipman, P.W., and Zoback, M.L., eds., *The Cordilleran Orogen: Coterminal U.S.*: Boulder, Colorado, Geological Society of America, *The Geology of North America*, v. G-3, p. 553-581.
- Wernicke, B., and Axen, G.J., 1988, On the role of isostasy in the evolution of normal fault systems: *Geology*, v. 16, p. 848-851.

